$CD4^+$ T cell responses in the spleen, reflecting the systemic compartment, and in Peyer's patches (PPs), reflecting the mucosal compartment (17). In addition, it has been demonstrated (18) that OVA-specific CTLs could be primed in C57BL/6 mice following oral exposure to a combination of OVA with CT, and specific cytotoxic activity was detected from spleen cells (SCs) only when they were restimulated in vitro with irradiated OVA-expressing syngeneic tumor cells, E.G7-OVA, which are OVA gene-transfected EL4 thymoma cells (19, 20). Also, intranasal preimmunization with OVA peptide (SIINFEKL) plus CT primed similar OVA-specific CTLs in the spleen of C57BL/6 mice, and the immunized mice were protected from the development of transferred E.G7-OVA (21).

Moreover, it has been shown that adoptive transfer of naive $CD8^+$ OVA-specific OT-I T cells into E.G7-OVA tumor-bearing syngeneic mice did not inhibit tumor growth, although adoptive transfer of preactivated OT-I CTL in vitro inhibited tumor growth in a dose-dependent manner (22). Furthermore, it has recently been reported that vaccination with dendritic cells (DCs) prepulsed ex vivo with CT-conjugated OVA (OVA-CT) gave rise to OVA-specific splenic $CD8^+$ T cells that produced IFN-γ, were cytotoxic to E.G7-OVA cells in vivo, and rejected already established in vivo E.G7-OVA tumors associated with high numbers of tumor-infiltrating $CD8^+$ T cells (23), indicating that the elimination of previously established tumor cells might require the infiltration of tumor-specific activated $CD8^+$ CTLs.

AQ: F

In the present study, we found two distinct types of $CD8\alpha\beta$-positive T cells among freshly isolated lymphocytes expressing OVA-specific TCRs, which can be detected by OVA peptide-bearing tetramers. One is in an activated effector state with cytotoxic activity and the other is a resting state and may gain cytotoxicity when stimulated with an OVA epitope peptide in vitro. Based on the observations, we defined direct cytotoxicity as the former state, in which freshly isolated and unstimulated CD8 T cells had specific cytotoxicity. Therefore, by comparing systemic SCs, we asked whether OVA-specific cytotoxic activity could be observed among freshly isolated IELs in mice orally administered OVA plus CT and examined whether those activated CTLs would reject or suppress the growth of already established tumors. Consequently, we observed dominant $TCR\alpha\beta$ and $CD8\alpha\beta$ OVA-specific CTL activities in freshly isolated IELs rather than in SCs after the oral administration of OVA plus CT, and such mucosal CTL activities could be expanded after oral boosting. Moreover, the growth of E.G7-OVA inoculated into the stomach or the epidermis was significantly suppressed, accompanied by the expansion of activated mucosal CTLs, and the infiltration of such OVA-specific $CD8\alpha\beta^+$ CTLs was observed in suppressed dermal tumor tissues. These results indicate that the growth of ongoing tumor cells can be suppressed in vivo by activated $CD8\alpha\beta$ CTLs with tumor-specific cytotoxicity via an orally administered tumor Ag with a suitable mucosal adjuvant.

## Materials and Methods

### *Mice*

Six- to 8-wk-old female C57BL/6 ($H\text{-}2^b$) mice were purchased from Charles River Japan, maintained in microisolator cages under pathogen-free conditions, and fed autoclaved laboratory chow and water. All animal experiments were performed according to guidelines for the care and use of laboratory animals set by the National Institutes of Health (NIH; Bethesda, MD) and approved by the Review Board of Nippon Medical School (Tokyo, Japan).

### *Oral and systemic immunization*

Chicken egg OVA, grade V (Sigma Aldrich), was dissolved in sterilized PBS. Mice were orally administered 100 mg of OVA or 10 μg of CT (List Biological Laboratories) alone or 100 mg of OVA plus 10 μg of CT, CTA, or CTB (List Biological Laboratories) in 0.3 ml of PBS. In some experiments, mice were orally administered 10 mg of OVA plus 10 μg of CT. For systemic immunization, mice were i.p. or s.c. injected with 100 mg of OVA or the same dose of OVA plus 10 μg of CT.

### *Preparation of IELs, lamina propria lymphocytes (LPLs), SCs, and tumor-infiltrating lymphocytes (TILs)*

IELs were prepared by the method described previously (12). In brief, after the small intestine, large intestine, or stomach was obtained from mice, fecal materials were flushed from the lumen with HBSS (Invitrogen Life Technologies) and connective tissues were carefully removed. The obtained guts were inverted and cut into several segments that were transferred to a 50-ml conical tube (Becton Dickinson Labware) containing 45 ml of HBSS with 5% FCS, 100 U/ml penicillin (Invitrogen Life Technologies), and 100 μg/ml streptomycin (Invitrogen Life Technologies). The tube was then shaken at 37°C for 45 min (horizontal position: orbital shaker at 150 rpm). Harvested cells from the intestinal epithelium were passed through a 10-ml syringe column containing loosely packed glass wool to remove tissue debris. Subsequently, the cells were suspended in 30% Percoll solution (Amersham Biosciences) and centrifuged for 20 min at 1,800 rpm. Cells at the bottom of the solution were then subjected to Percoll discontinuous gradient centrifugation for 20 min at 1,800 rpm and IELs were recovered at the interphase of 44 and 70% Percoll solutions. LPLs were prepared by the method described previously (24). In brief, after the small intestine, large intestine, or stomach was dissected from mice, fecal material was flushed from the lumen with HBSS and PPs were carefully removed. The obtained guts were inverted and cut into several segments that were transferred to a 50-ml conical tube containing 45 ml of HBSS with 5% FCS and 1 mM EDTA (Wako Pure Chemical Industries). The tube was shaken at 37°C for 45 min (horizontal position; orbital shaker at 150 rpm). The gut segments were then washed with PBS and shaken in 40 ml of HBSS with 5% FCS and 0.1 mg/ml collagenase (Sigma-Aldrich) at 37°C for 45 min (horizontal position; orbital shaker at 60 rpm). Harvested cells were passed through a nylon mesh and suspended in 40% Percoll solution, and then 70% Percoll solution was underlain. The solution was centrifuged for 20 min at 1,800 rpm and LPLs were recovered at the interphase of 40 and 70% Percoll solutions. These procedures provided >95% viable lymphocytes with a cell yield of $5–10 \times 10^6$ of small intestinal IELs, $2–3 \times 10^5$ of large intestinal IELs, $7–12 \times 10^3$ of gastric IELs, $4–9 \times 10^5$ of small intestinal LPLs, $1–3 \times 10^5$ of large intestinal LPLs, or $5–9 \times 10^4$ of gastric LPLs per mouse. The cells were suspended in complete T cell medium (25) composed of RPMI 1640 medium (Sigma-Aldrich) supplemented with 2 mM L-glutamine (ICN Biomedicals), 1 mM sodium pyruvate (Invitrogen Life Technologies), 0.1 mM nonessential amino acid (Invitrogen Life Technologies), a mixture of vitamins (ICN Biomedicals), 1 mM HEPES (Invitrogen Life Technologies), 100 U/ml penicillin (Invitrogen Life Technologies), 100 μg/ml streptomycin (Invitrogen Life Technologies), 50 μM 2-ME (Sigma-Aldrich), and heat-inactivated 10% FCS. For TIL preparation, tumors were removed from mice, incubated in 1 mg/ml collagenase (Wako Pure Chemical Industries) with PBS at 37°C for 1 h, and crushed gently. TILs were prepared using Percoll solutions as described in the previous paragraph regarding IEL preparation. The spleen was aseptically removed and a single cell suspension was prepared. For osmotic hemolysis, single cells were suspended in 0.1× PBS and an equal amount of 2× PBS was added immediately. To enrich IELs, LPLs, and TILs from mice, the interface between the 40 and 70% Percoll solutions (26), in which NK cells and unfractionated SCs, which may also include NK cells, must be included, was collected.

AQ: G

### *Flow cytometry analysis*

Cells were double-stained with PE-labeled $H\text{-}2K^b$/OVA tetramer-SIINFEKL (Beckman Coulter) or $H\text{-}2K^b$/PB1 tetramer-SSYRRPVGI (Medical & Biological Laboratories) and FITC-labeled anti-mouse TCRβ, CD8α (BD Pharmingen), or CD8β (Caltag Laboratories). Peptide PB1 703–711, SSYRRPVGI, for the control tetramer was derived from influenza virus (27). Dead cells were determined using 7-aminoactinomycin D viability dye (Beckman Coulter) and stained cells were analyzed by FACScan using the CellQuest program (BD Biosciences).

### *In vitro restimulation of SCs or IELs with E.G7-OVA*

Lymphocytes were restimulated in vitro by the method described previously (19). Freshly isolated SCs ($3 \times 10^7$) or IELs ($3 \times 10^7$) were restimulated with $3 \times 10^6$ irradiated (20,000 rad) E.G7-OVA cells (19, 20) ($H\text{-}2^b$; American Type Culture Collection) in 10 ml of complete T cell medium per upright 25-$cm^2$ flask in 5% $CO_2$ at 37°C for 6 days. Six days later, the viability of the lymphocytes was 35–51% in SCs and 16–26% in IELs. The

in vitro restimulated cells were collected and their OVA-specific cytotoxicity was measured by the following procedure.

### *CTL assay*

For the CTL assay, freshly isolated IELs, SCs, or TILs were used. Cytolytic activity was measured using a standard $^{51}$Cr-release assay as previously described (12). In brief, various numbers of effector cells were incubated with $3 \times 10^3$ $^{51}$Cr-labeled targets for 6 h at 37°C in 200 μl of RPMI 1640 medium containing 10% FCS in round-bottom 96-well cell culture plates (BD Biosciences). After incubation, the plates were centrifuged for 10 min at $330 \times g$, and 100 μl of cell-free supernatants were collected to measure radioactivity with a Packard Auto-Gamma 5650 counter (Hewlett-Packard Japan). Maximum release was determined from the supernatant of cells that had been lysed by the addition of 5% Triton X-100, and spontaneous release was determined from target cells incubated without added effector cells. The percentage of specific lysis was calculated as 100 × (experimental release − spontaneous release)/(maximum release − spontaneous release). SEs of the means of triplicate cultures were always <5% of the mean. Each experiment was performed at least three times.

### *Measurement of in vivo antitumor effects*

E.G7-OVA cells ($5 \times 10^6$), OVA gene-transfected EL4 thymoma cells (19, 20), were implanted into the gastric or dermal tissue of syngeneic C57BL/6 mice (H-2$^b$). For tumor implantation into the gastric tissue, mice were anesthetized and underwent an abdominal operation and then E.G7-OVA cells in 50 μl of RPMI 1640 were injected into the muscle layer of the stomach using a syringe with a 29-gauge needle (Terumo). For implantation into the dermal tissue, mice were anesthetized and E.G7-OVA cells in
AQ: H 100 μl of RPMI 1640 were injected intradermally by a 29-gauge needle syringe. On day 3 after implantation into the gastric or dermal tissue, when the tumor mass became visible, tumor-bearing mice were orally or systemically administered OVA plus CT as described above. Seven days after the first administration, some of the mice were similarly boosted with the same materials. The growing tumors implanted into the gastric or dermal tissues were followed by measuring the length ($a$) and width ($b$), the and tumor volume ($V$) was calculated according to the formula $V = ab^2/2$ as reported previously (28). When the longer axis of each tumor was >20 mm, all mice were anesthetized and sacrificed according to the guidelines for the care and use of laboratory animals set by the NIH.

### *Histological analysis of tumor tissues*

Freshly excised tumor tissues were embedded in Tissue-Tek OCT compound (Sakura Finetek) at −80°C. Tissue segments were sectioned at 6 μm using a cryostat. Sections were placed on a poly-L-lysine-coated glass slide, air dried, and then fixed in 10% formalin PBS for 5 min and stained with H&E. For immunohistochemical staining, sections were fixed in cold acetone for 5 min and incubated with blocking solution (Block-ace: Dainippon Pharmaceutical) for 30 min at 37°C and then incubated with biotin-conjugated rat anti-CD8β Ab (Caltag Laboratories) or control isotype-matched rat IgG2a Ab (Caltag Laboratories) overnight at 4°C. Endogenous peroxidase was quenched by incubation in 0.3% $H_2O_2$ and 0.1% $NaN_3$ in distilled water for 10 min. The sections were incubated with avidin-biotin peroxide complexes (Vectastain ABC kit; Vector Laboratories) followed by color reaction with a Vectastain diaminobenzidine substrate kit (Vector Laboratories).

### *Statistical analysis*

Student's $t$ test was used to determine the statistical significance of differences between groups in tumor growth. Data were considered significant at $p < 0.05$.

## Results

### *Priming of OVA-specific CD8αβ-positive CTLs with direct cytotoxicity via oral administration with OVA plus CT*

It has been reported that OVA-specific CTLs could be primed in C57BL/6 mice by oral or i.v. immunization with OVA plus CT together with nontoxic CTB, and specific cytotoxic activity was detected from immune SCs only when they were restimulated in vitro with irradiated OVA-expressing syngeneic tumor (E.G7-OVA) cells (18). It has also been shown that activated CTLs but not naive primed CTLs could represent antitumor responses in vivo (22). Similarly, we have recently observed in HIV-1-specific CTL-TCR transgenic mice that activated CTLs but not freshly isolated TCR-bearing CD8αβ-positive T cells showed specific cytotoxicity, and the most critical sites for activating TCR-bearing CD8αβ T cells were mucosal compartments when Tg mice were administered a specific Ag for TCR (12).

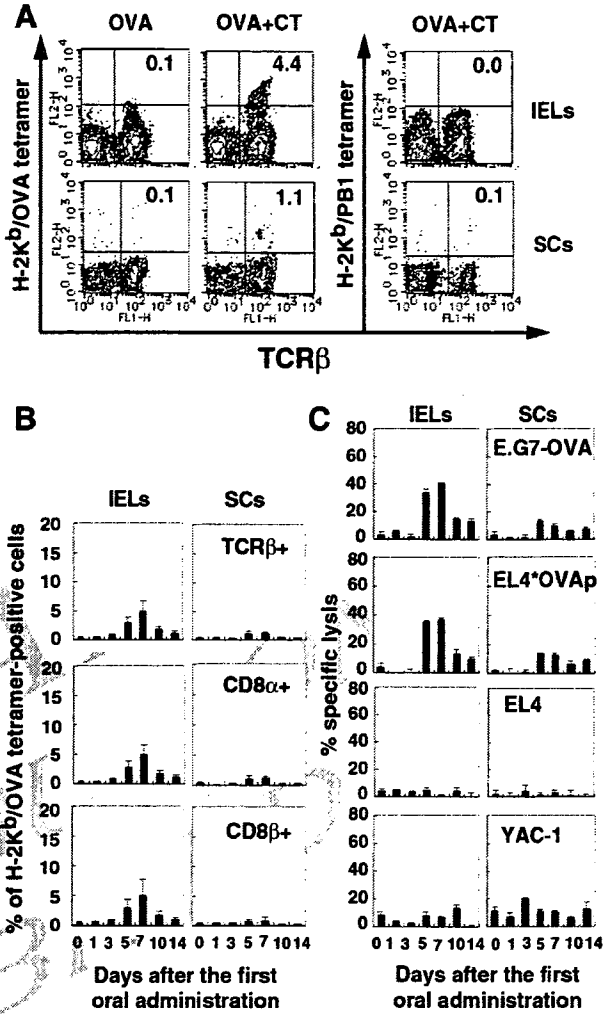


**FIGURE 1.** Analysis of OVA-specific direct cytotoxicities in IELs and SCs after primary immunization with OVA plus CT. *A*, Analysis of H-2K$^b$/OVA tetramer-positive cells. C57BL/6 mice were orally administered OVA or OVA plus CT once. IELs and SCs were collected from mice 5 days after the first oral administration, stained with either PE-labeled H-2K$^b$/OVA tetramer-SIINFEKL or H-2K$^b$/PB1 tetramer-SSYRRPVGI together with FITC-labeled anti-mouse TCRβ, and analyzed by flow cytometry. Each value represents the percentage of cells expressing both indicated markers. Data are representative of three independent experiments. *B*, Kinetics of H-2K$^b$/OVA tetramer-positive cells after primary immunization. C57BL/6 mice were orally administered OVA plus CT once. IELs and SCs were collected from mice at various days after the first oral administration, stained with PE-labeled H-2K$^b$/OVA tetramer together with FITC-labeled anti-mouse TCRβ, CD8α, or CD8β, and analyzed by flow cytometry. The results are shown as the mean ± SD of four mice. *C*, Kinetics of OVA-specific direct cytotoxic responses. C57BL/6 mice were orally primed and cells were collected as described in *B*. OVA-specific CTL responses were measured by $^{51}$Cr-release assay using E.G7-OVA cells (H-2$^b$), YAC-1 cells, and EL4 cells (H-2$^b$) pulsed with or without 4 μM OVA-peptide, SIINFEKL, as target cells. E:T ratio was 100:1. The results shown as the mean ± SD in triplicate of pooled cells from two mice are representative of three independent experiments.

These findings prompted us to examine whether direct OVA-specific cytotoxic activity could be induced among IELs in mice AQ: I

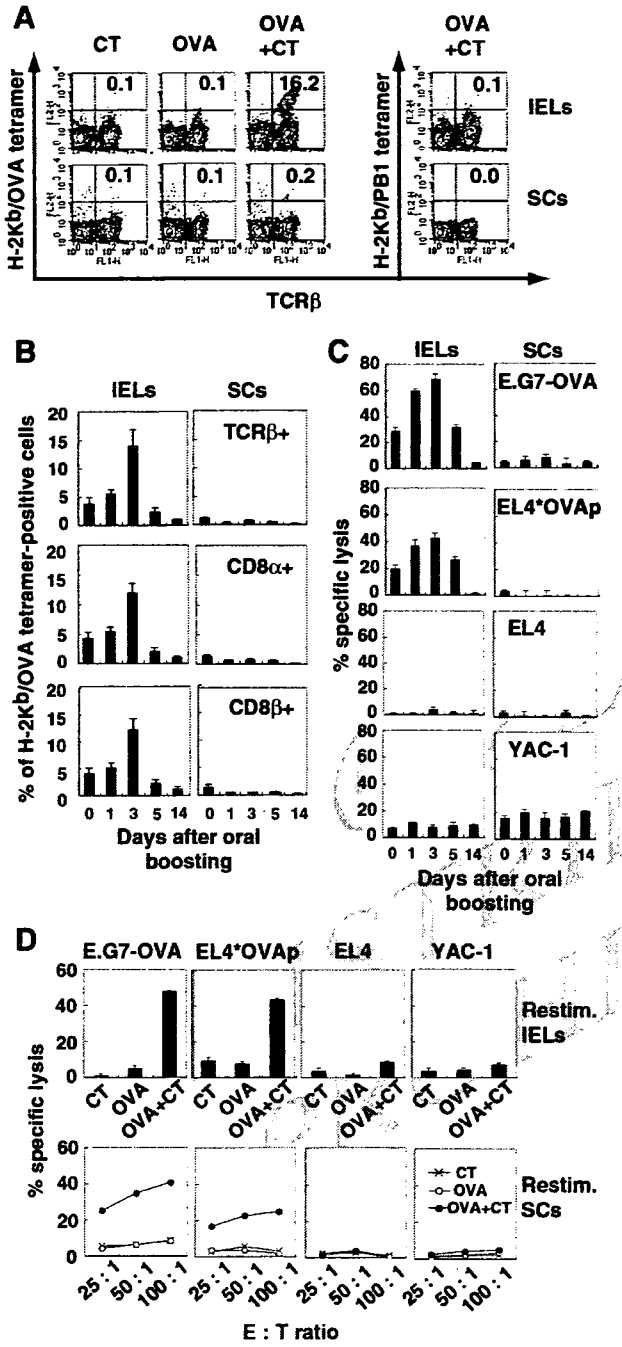


FIGURE 2. Expansion of direct OVA-specific cytotoxicities after oral boosting with OVA plus CT. *A*, Activated H-2K$^b$/OVA tetramer-positive cells after oral boosting. C57BL/6 mice were orally administered CT, OVA, or OVA plus CT once weekly for 2 wk. IELs and SCs were collected from mice 3 days after the second oral boost and stained with PE-labeled H-2K$^b$/OVA tetramer or H-2K$^b$/PB1 tetramer together with FITC-labeled anti-mouse TCR$\beta$. Each value represents the percentage of cells expressing both indicated markers. Data are representative of three independent experiments. *B*, Kinetics of H-2K$^b$/OVA tetramer-positive cells after oral boosting. C57BL/6 mice were orally administered OVA plus CT once weekly for 2 wk. IELs and SCs were collected from mice at various days after the second oral boost, stained with PE-labeled H-2K$^b$/OVA tetramer together with FITC-labeled anti-mouse TCR$\beta$, CD8$\alpha$, or CD8$\beta$, and analyzed by flow cytometry. The results are shown as the mean ± SD of four mice. *C*, Kinetics of the secondary expansion of OVA-specific direct CTL responses. C57BL/6 mice were treated orally and the cells were collected as described in *B*. OVA-specific CTL responses were measured by $^{51}$Cr-release assay using E.G7-OVA cells, YAC-1 cells, and EL4 cells pulsed with or without OVA peptide as targets. The E:T ratio is 100:1. The results shown as the mean ± SD in triplicate of pooled cells from two mice are representative of three independent experiments. *D*, Activation of OVA-specific CTLs by in vitro restimulation (Restim.). C57BL/6 mice were orally administered CT, OVA, or OVA plus CT once weekly for 2 wk. IELs ($3 \times 10^7$) and SCs ($3 \times 10^7$) were collected from mice 9 days after the second oral boost, and cocultured with $3 \times 10^6$ irradiated E.G7-OVA. Six days later, OVA-specific lysis of stimulated IELs and SCs was measured by $^{51}$Cr-release assay. The E:T ratio is 100:1 in IELs and 100:1, 50:1, or 25:1 in SCs. The results are shown as the mean ± SD in IELs or the mean in SCs in triplicate of pooled cells from two mice. Data are representative of three independent experiments.

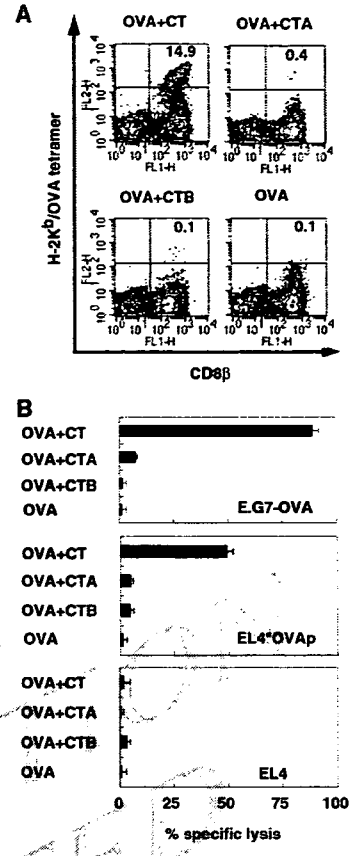


FIGURE 3. Both subunits, CTA and CTB, are essential for the induction of OVA-specific CTLs. C57BL/6 mice were orally administered OVA or OVA plus intact CT, CTA subunit or CTB subunit once weekly for 2 wk. IELs were collected from mice 3 days after the second oral administration. *A*, IELs were stained with PE-labeled H-2K$^b$/OVA tetramer and FITC-labeled anti-mouse CD8$\beta$. Each value represents the percentage of cells expressing both indicated markers. *B*, OVA-specific CTL responses of isolated IELs were measured by $^{51}$Cr-release assay using E.G7-OVA cells, EL4 cells pulsed with or without OVA peptide as targets. The E:T ratio is 100:1. Data are shown as the mean ± SD in triplicate of pooled cells from two mice. The results are representative of three independent experiments for both *A* and *B*.

AQ: P

administered OVA plus CT orally without requiring in vitro restimulation. To carry out this experiment, we used a H-2K$^b$/OVA tetramer to detect cells expressing OVA-specific TCR in freshly isolated IELs as well as in the SCs of primed mice 5 days after immunization. Also, to evaluate the purity of IELs, CD103 (integrin

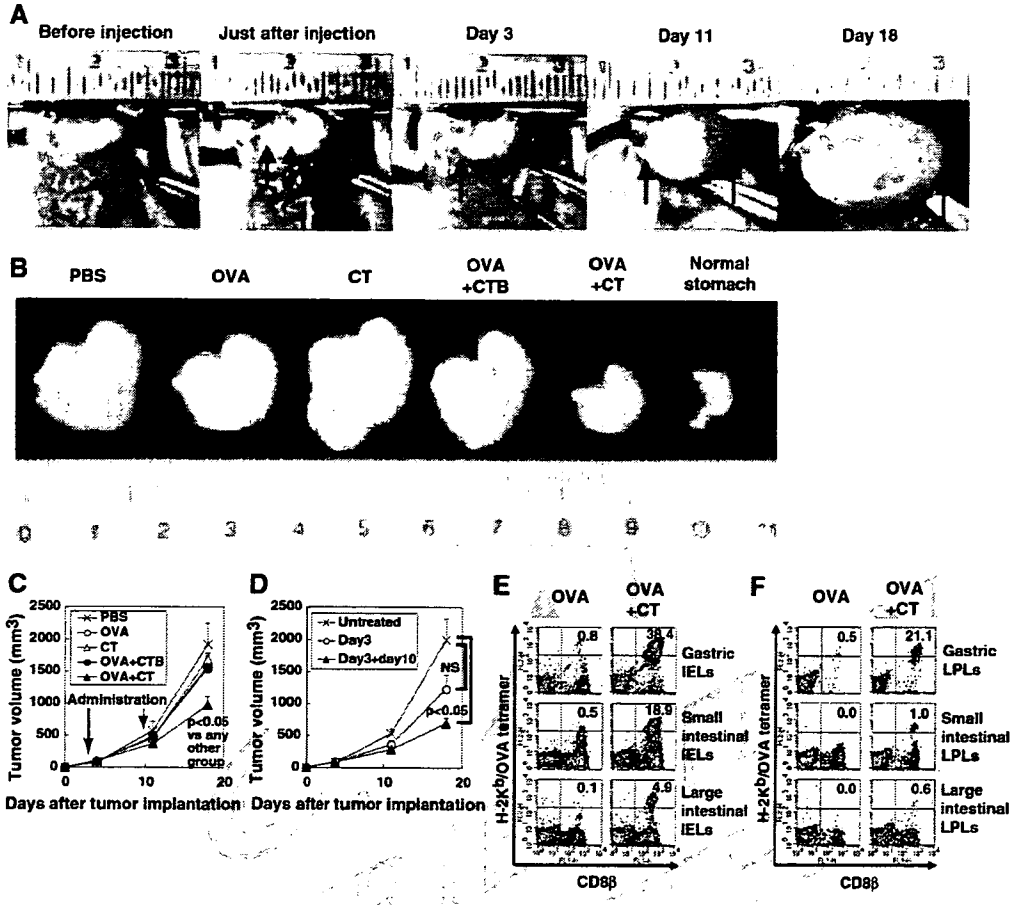


**FIGURE 4.** Suppression of the growth of a tumor implanted into gastric tissue by oral administration of OVA plus CT. *A*, Growth of visible tumor after implantation of E.G7-OVA cells into gastric tissue. C57BL/6 mice were implanted with $5 \times 10^6$ E.G7-OVA cells into the muscle layer of the stomach. Each day, the same mice were anesthetized and underwent an abdominal operation, and tumors were observed. Arrows point to both ends of the longer axis in the tumor. *B*, C57BL/6 mice were implanted with $5 \times 10^6$ E.G7-OVA cells into the muscle layer of the stomach. Three days later, tumor-bearing mice were orally administered PBS, OVA, CT, OVA plus CTB subunit, or OVA plus CT. Seven days later, the second oral administration was performed in the same manner. Stomachs were excised from the mice 18 days after tumor implantation, as well as from untreated, normal mice. *C*, Tumor volumes were calculated based on the formula described in *Materials and Methods*, and the results are shown as the mean ± SEM. The results were obtained from 9–13 mice per group. $p < 0.05$ indicates statistically significant difference between OVA plus CT (▲) and any other groups. *D*, C57BL/6 mice were implanted with E.G7-OVA cells in the stomach. Three days later, tumor-bearing mice were orally administered OVA plus CT or left untreated. Seven days later, some orally immunized mice were boosted in the same manner or left untreated. The results are shown as the mean ± SEM of 5–7 mice per group. $p < 0.05$ and NS indicate statistically significant and not significant differences, respectively, between the boosted (▲) and nonboosted (○) groups and the untreated group (×). *E* and *F*, Induction of CD8β and H-2K$^b$/OVA tetramer-positive cells in IELs (*E*) and LPLs (*F*) of the stomach, small intestine, or large intestine after oral administration of OVA plus CT. C57BL/6 mice were orally administered OVA or OVA plus CT once weekly for 2 wk. IELs and LPLs were collected from mice 3 days after the second oral administration. Cells were stained with PE-labeled H-2K$^b$/OVA tetramer and FITC-labeled anti-mouse CD8β. Each value represents the percentage of cells expressing both indicated markers. The results are representative of three independent experiments.

α-IEL chain)-positive cells in the collected samples were examined by flow cytometry. CD103 is highly expressed on >90% of IELs (29, 30) but on only 15% of SCs (31). In the present study, CD103-positive cells occupied >90% of IELs and ~15% of SCs (data not shown). Although a small number of OVA-specific TCR-expressing cells were detected in both IELs (4.5–5.0%) and SCs (1.0–1.5%) after oral administration of OVA plus CT in comparison with control H-2K$^b$/PB1-positive cells, H-2K$^b$/OVA tetramer-positive cells were not observed in mice treated with OVA alone (Fig. 1*A*). Such OVA peptide-specific TCR-expressing cells were TCRγδ negative (data not shown) and both CD8α and β positive (Fig. 1*B*). The number of tetramer-positive cells, to which the magnitude of direct OVA-specific cytotoxicity closely corresponded, was maximal at day 7 after oral immunization with both IELs and SCs (Fig. 1*B*), but it did not correspond to NK cell activity as measured against YAC-1 targets (Fig. 1*C*). The results clearly demonstrate that direct OVA-specific CTL cytotoxicity is dominantly observed in mucosal IELs after primary oral administration of OVA plus CT.

*Augmentation and kinetics of direct OVA-specific cytotoxicity by CD8αβ CTLs among IELs and SCs via oral boosting with OVA plus CT at day 7 after the primary administration*

As shown above, because only 4.5–5.0% of IELs were temporarily activated by a one-shot oral administration, we extensively examined the effect of oral boosting with OVA plus CT at various days after primary immunization. The number of H-2K$^b$/OVA tetramer-positive cells was significantly enhanced among IELs but not among SCs when primed mice were boosted (Fig. 2*A*). Such an effect was highest when mice were boosted at day 7 after initial

priming (data not shown). Tetramer-positive cells were again
AQ: K TCRβ-, CD8α-, and CD8β-positive IELs and their number peaked at day 3 after boosting (Fig. 2*B*). Correspondingly, direct OVA-specific cytotoxicity was greatly enhanced among IELs and the maximal cytotoxicity of IELs was observed at day 3 after boosting (Fig. 2*C*), although such direct cytotoxicity appeared to be completely lost in SCs (Fig. 2*C*). Nonetheless, SCs showed good epitope-specific cytotoxicity similar to that of IELs when they were restimulated in vitro with irradiated E.G7-OVA (Fig. 2*D*), suggesting that the priming effect by the oral administration of OVA plus CT also remained in systemic SCs.

It should be noted that the memory of OVA-specific CTLs persisted among IELs but not SCs. When secondary boosting with OVA plus CT was performed even 6 mo after primary boosting at day 7, the number of H-2K$^b$/OVA tetramer-positive cells was still detected at ~6% in IELs, and they showed remarkable direct cytotoxicity of ~84.5% against E.G7-OVA cells and 58.4% against EL4 cells pulsed with OVA peptide 3 days after secondary boosting (data not shown). Again, we could not detect any measurable direct cytotoxicity in the SCs of secondary boosted mice (data not shown).

### *Both CTA and CTB subunits are required to induce direct OVA-specific cytotoxicity in IELs*

CT is comprised of a single A subunit, CTA, and five B subunits, CTB. When OVA was administered orally to mice with either 10 μg of CTA or an equal amount of CTB, H-2K$^b$/OVA tetramer-positive cells as well as direct OVA-specific cytotoxicity could not
F3 be detected in IELs (Fig. 3, *A* and *B*) and SCs (data not shown), although a significant number of tetramer-positive cells and strong direct OVA-specific cytotoxicity were observed among IELs of mice administered orally with OVA plus 10 μg of intact CT (Fig. 3, *A* and *B*). Even when using 50 μg of CTA or CTB for the administration of OVA, direct cytotoxicity was not observed (data not shown); therefore, both CTA and CTB subunits are required to induce direct Ag-specific cytotoxicity.

### *Effects of oral administration and booting with OVA plus CT on OVA-expressing tumor growth established in the stomach*

We then examined in vivo antitumor effects of oral administration with tumor Ag plus CT on already established tumors growing in mice. C57BL/6 mice were implanted with 5 × 10$^6$ syngeneic
F4 E.G7-OVA cells into the muscle layer of the stomach (Fig. 4*A*). Three days later, tumor-bearing mice (Fig. 4*A*) were orally administered various combinations of OVA plus adjuvant and boosted with the same materials 7 days after the initial oral administration. To our surprise, tumor growth in the stomach of mice orally administered OVA plus CT twice was visually (Fig. 4*B*) and significantly ($p < 0.05$; Fig. 4*C*) suppressed on day 18 after tumor implantation as compared with other control groups such as OVA plus CTB or CT alone. However, when tumor-bearing mice were orally administered OVA plus CT once and without boosting, no statistically significant suppression was observed on day 18 as compared with untreated control mice, although a slight suppressive effect could be seen (Fig. 4*D*). Therefore, two oral administrations of tumor-Ag plus CT with an appropriate interval induced significant ongoing tumor suppression.

As previously shown, direct OVA-specific cytotoxicity among small intestinal IELs was greatly enhanced after boosting with OVA plus CT (Fig. 2, *A*, *B*, and *C*). We also examined whether direct OVA-specific CTLs were induced in the IELs and LPLs of the stomach, small intestine, and large intestine from boosted mice in which gastric tumor growth was significantly suppressed. We observed an increase in the number of H-2K$^b$/OVA tetramer-positive

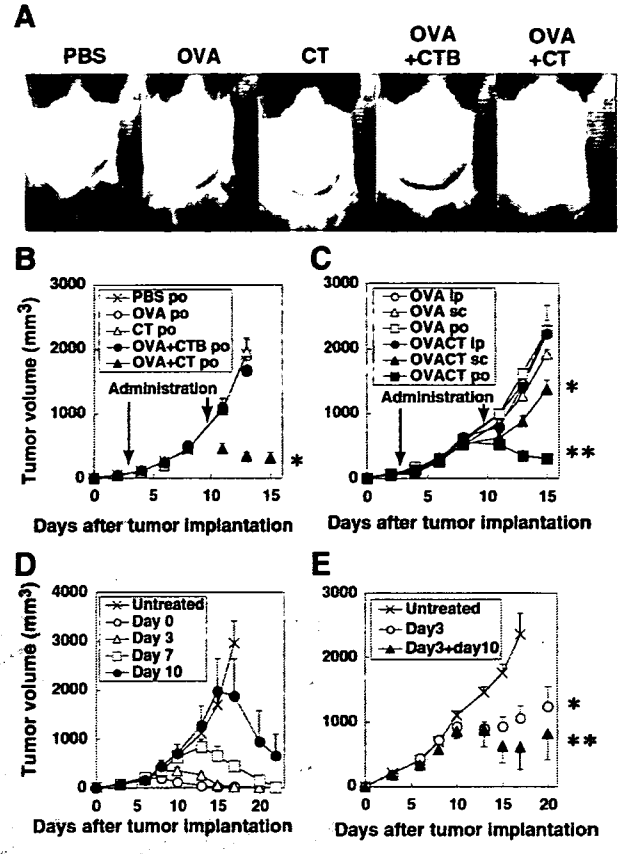


**FIGURE 5.** Suppression of intradermal tumor growth by oral administration with OVA plus CT. C57BL/6 mice were implanted intradermally with 5 × 10$^6$ E.G7-OVA cells. Three days later, tumor-bearing mice were orally administered PBS, OVA, CT, OVA plus CTB subunit, or OVA plus CT. Seven days later, the second oral administration was performed in the same manner. *A*, Visual suppressive effect of oral inoculation of OVA plus CT on dermal tumor growth. *B*, Tumor volumes were calculated based on the formula described in *Materials and Methods* and the results are shown as the mean ± SEM. Results were obtained from 5–6 mice per group. The asterisk (*) indicates statistically significant difference between the OVA plus CT group (closed triangle) and any other group at 11 days ($p < 0.05$) and 13 days ($p < 0.005$) after tumor inoculation. *C*, C57BL/6 mice were implanted intradermally with E.G7-OVA cells. Three days later, tumor-bearing mice were intraperitoneally (ip), subcutaneously (sc), or orally (po) administered OVA alone or OVA plus CT. Seven days later, the second treatment was performed in the same manner. The results are shown as the mean of tumor volumes ± SEM. Results were obtained from 5–6 mice per group. The asterisk (*) shows statistically significant differences ($p < 0.05$) between the s.c. OVA plus CT group (▲) and the s.c. OVA alone group at days 11, 13, and 15 after tumor implantation, and the two asterisks (**) indicate significant differences ($p < 0.01$) between the oral OVA plus CT group (■) and the oral OVA alone group on the same days. *D*, C57BL/6 mice were implanted intradermally with E.G7-OVA cells. The mice were orally administered once with OVA plus CT at day 0, 3, 7, or 10 after tumor implantation. The results are shown as the mean of tumor volumes ± SEM. Results were obtained from 10–12 mice per group. In single orally administered groups, significant tumor regression ($p < 0.05$) was observed at 7 days after oral administration compared with the untreated group. *E*, C57BL/6 mice were implanted intradermally with E.G7-OVA cells. Three days later, tumor-bearing mice were orally administered a low dose (10 mg) of OVA plus CT. Seven days later, some orally administered mice were boosted in the same manner. The results obtained from 5- mice per group are shown as the mean of tumor volumes ± SEM. The asterisk (*) indicates statistically significant differences ($p < 0.01$) between the nonboosted (○) and untreated mice (×) groups at days 15 and 17 after tumor implantation, and the two asterisks (**) indicate significant differences ($p < 0.005$) between the boosted (▲) and untreated groups on the same days.

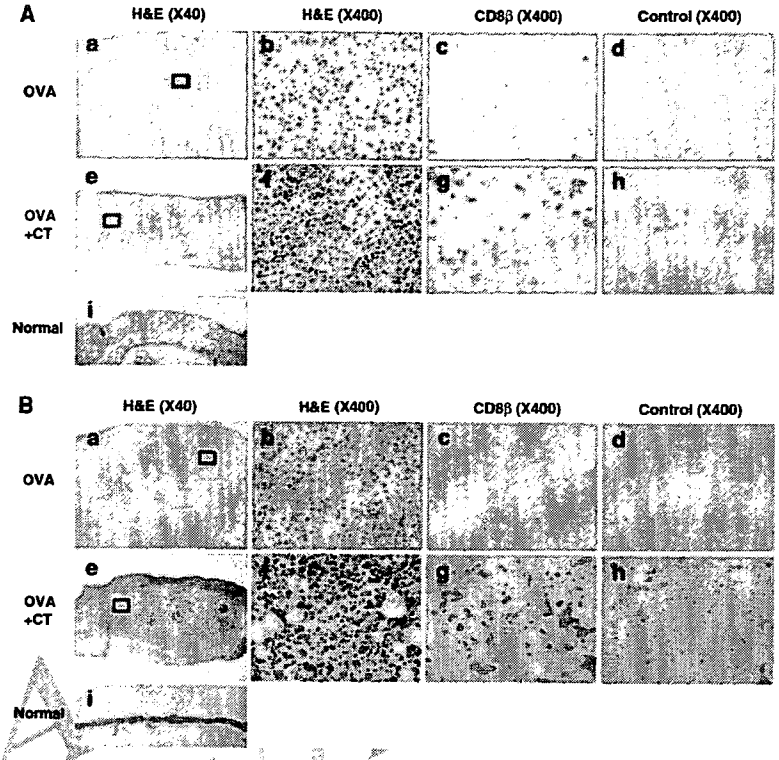


**FIGURE 6.** Infiltration of CD8$\alpha\beta$ positive lymphocytes into tumor tissues in mice orally administered OVA plus CT. C57BL/6 mice were implanted with $5 \times 10^6$ E.G7-OVA cells into the muscle layer of the stomach (*A*, *a–h*) or skin (*B*, *a–h*). Three days later, tumor-bearing mice were orally administered OVA (*A*, *a–d*, and *B*, *a–d*) or OVA plus CT (*A*, *e–h* and *B*, *e–h*). Seven days later, the second oral administration was performed in the same manner. Gastric and dermal tumor tissues were removed from mice 3 days after the second oral boost. Frozen sections of tumor tissues and normal tissues were prepared and stained with H&E (*A*, *a*, *b*, *e*, *f*, and *i* and *B*, *a*, *b*, *e*, *f*, and *i*) or immunohistochemically stained with biotin-conjugated rat anti-CD8$\beta$ mAb (*A*, *c* and *g*, and *B*, *c* and *g*) or control isotype-matched rat IgG2a Ab (*A*, *d* and *h*, and *B*, *d* and *h*). Image magnification is either ×40 (*A*, *a*, *e*, and *i* and *B*, *a*, *e*, and *i*) or ×400 (*A*, *b–d* and *f–h* and *B*, *b–d* and *f–h*). *A*, *b* and *f* and *B*, *b* and *f* are enlarged images (×400) of the squared areas in the images (×40) of *A*, *a* and *e* and *B*, *a* and *e*, respectively.

cells among IELs in the stomach (38.4%) as well as the small (18.9%) and large intestine (4.9%) of tumor-suppressed mice (Fig. 4*E*) and also among LPLs in the stomach (21.1%) as well as the small (1.0%) and large (0.6%) intestine (Fig. 4*F*). Thus, the ability of LPLs to suppress tumor growth may be weaker than that of IELs. The results suggest that oral administration of Ag plus intact CT with appropriate mucosal boosting apparently suppressed the already established tumor growth in gastric tissue, particularly after oral boosting, probably through the activation of Ag-specific CTLs in the mucosal compartment.

*Effects of oral administration and boosting with OVA plus CT on already established OVA-expressing dermal tumor growth*

Next, we investigated the effect of the oral administration of tumor Ag plus CT on tumor growth in the skin, where the digestive tract is not directly associated. Mice were implanted with $5 \times 10^6$ E.G7-OVA cells intradermally. Three days later, tumor-bearing mice were orally administered various combinations of OVA plus adjuvant and boosted with the same materials 7 days after the initial oral administration. Interestingly, intradermal tumor growth was again strongly suppressed visually 11 days after tumor implantation in the dermis of mice orally administered OVA plus CT as compared with various other groups (Fig. 5*A*). This visual effect was confirmed by calculating the volume of the tumors established at day 11 and day 13 in each group ($p < 0.05$ and $p < 0.005$, respectively; Fig. 5*B*). We also examined the effect of the administration of tumor Ag plus CT via various routes on intradermal tumor growth. Although a slight suppression was observed by s.c. inoculation of OVA plus CT, tumor growth was not suppressed at all by i.p. administration in comparison with the oral treatment group (Fig. 5*C*). It should be noted that tumor growth in the dermis was markedly suppressed even by a single oral administration of OVA plus CT on day 0, 3, 7, or 10 after tumor implantation (Fig. 5*D*). In each group, tumor growth was suppressed ($p < 0.05$) and the tumor volume was small around 7 days after oral administration. Unexpectedly, there was almost no difference in the suppressive effects on tumor growth between mice treated with a single administration and boosted mice showing much stronger direct cytotoxicity (data not shown). However, when the dosage quantity of OVA was decreased by one-tenth, tumor growth in boosted mice was more significantly ($p < 0.005$) suppressed than in nonboosted mice ($p < 0.01$; Fig. 5*E*). Collectively, the results indicate that the oral administration of tumor Ag plus CT with appropriate mucosal boosting may induce a remarkable suppression of already established tumor growth in the skin via mucosally generated CTLs.

*Infiltration of CD8$\alpha\beta$-positive cells in suppressed tumor tissues*

We thus examined whether OVA-specific CD8$\alpha\beta$-positive CTLs were actually seen in suppressed tumor tissues such as the stomach and dermis. To determine tumor-infiltrating CD8$\alpha\beta^+$ cells, immunohistochemical staining was performed using biotin-conjugated rat anti-CD8$\beta$ Ab (Fig. 6*A*, *c* and *g* and *B*, *c* and *g*) or control isotype-matched rat IgG2a Ab (Fig. 6*A*, *d* and *h* and *B*, *d* and *h*). Indeed, although mononuclear cells were seen in the gastric tumor tissues of mice treated with OVA alone, CD8$\alpha\beta$-positive cells were not observed at all (Fig. 6*A*, *a–d*). In contrast, infiltration of inflammatory mononuclear cells together with CD8$\alpha\beta$-positive cells was observed in suppressed gastric tumor tissues (Fig. 6*Ag*). As shown in Fig. 6*Ai*, normal gastric tissue is composed of the epithelium, lamina propria, lamina muscularis mucosae, muscle layer, and serosa from the inside surface in sequence. As compared with normal gastric tissue, a great number of large tumor cells (EG.7-OVA) were mainly found between the lamina muscularis mucosae and serosa of tumor-implanted tissues (Fig. 6*A*, *a* and *b*) and the infiltration of tumor cells into the lamina propria over the lamina muscularis mucosae was also observed (data not shown). However, in suppressed gastric tumor tissues (Fig. 6*Ae*) the tumor cell layer under the lamina muscularis mucosae was markedly thinner than that of an unsuppressed tumor (Fig. 6*Aa*), in which

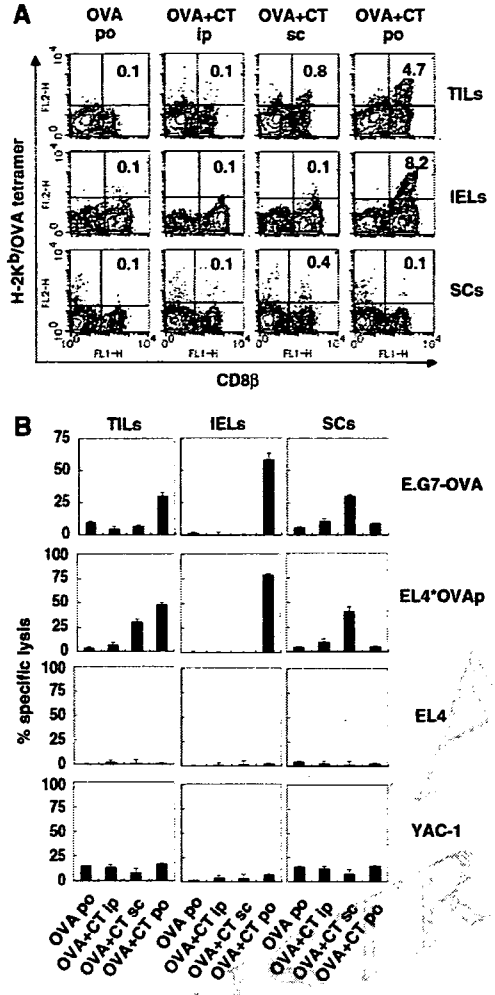


**FIGURE 7.** Detection of OVA-specific CTLs in TILs. C57BL/6 mice were implanted intradermally with E.G7-OVA cells. Three days later, mice were orally (po), subcutaneously (sc), or intraperitoneally (ip) administered OVA plus CT or orally treated with OVA. Seven days later, the second oral administration was performed in the same manner. TILs, IELs, and SCs were collected from mice 3 days after the second oral administration. *A*, TILs, IELs and SCs were double stained with PE-labeled H-2K$^b$/OVA tetramer and FITC-labeled anti-mouse CD8$\beta$. *B*, OVA-specific CTL responses of TILs, IELs, and SCs were measured by a $^{51}$Cr-release assay using E.G7-OVA cells, YAC-1 cells, and EL4 cells pulsed with or without OVA peptide as targets. The E:T ratio is 5:1 in TILs, or 100:1 in IELs and SCs. The results are shown as the mean ± SD in triplicate of pooled cells from three mice. The results are representative of three independent experiments.

tumor cells almost never infiltrated the lamina propria over the lamina muscularis mucosae. Similarly, as for dermal tumor tissues, mononuclear cells together with CD8$\alpha\beta$-positive cells were not observed in mice treated with OVA alone (Fig. 6*B*, *a–d*), whereas the infiltration of a large number of mononuclear cells and CD8$\alpha\beta$-positive cells was observed in suppressed dermal tumor tissues (Fig. 6*B*, *e–g*). Dermal tumor sections were not stained with control isotype-matched rat IgG (Fig. 6*B*, *d* and *h*). As shown in Fig. 6*Bi*, normal skin is composed of epidermides and dermis from the surface in sequence. In tumor cell-implanted dermal tissues, although the infiltration of mononuclear cells or CD8$\alpha\beta$-positive cells was not observed, many large tumor cells were found thickly beneath the epidermides (Fig. 6*B*, *a* and *b*); however, when tumor cell-implanted mice were treated with OVA plus CT, most tumor cells became necrotic or apoptotic (Fig. 6*B*, *e* and *f*).

*Measurement of tumor-specific cytotoxic activity by tumor-infiltrating cells in tumor-suppressed mice*

To confirm whether infiltrated CD8$\alpha\beta$-positive T cells achieved OVA-specific cytotoxicity, we isolated TILs containing both mononuclear cells and CD8$\alpha\beta$-positive T cells from suppressed dermal tumor tissues as well as from their IELs and SCs. As expected, the number of H-2K$^b$/OVA tetramer-positive cells increased in both the TILs and IELs but not in the SCs of mice bearing suppressed tumors induced by oral administration with OVA plus CT as compared with mice inoculated with OVA plus CT via another route (Fig. 7*A*), and those increased tetramer-positive cells showed significant direct OVA-specific CTL activity (Fig. 7*B*). It should be noted that, although the number of increased cells specific for the H-2K$^b$/OVA tetramer was small in mice inoculated with OVA plus CT s.c., both the TILs (0.8%) and the SCs (0.4%) but not the IELs (0.1%) of the mice represented a detectable level of direct OVA-specific cytotoxicity (Fig. 7*B*). These findings suggest that s.c. immunization with Ag plus CT may preferably activate systemic (splenic) Ag-specific CTLs rather than local (intraepithelial) CTLs. Moreover, NK cell cytotoxicity determined against YAC-1 cells was not observed in TILs, IELs, and SCs by oral, s.c., or i.p. immunization of OVA plus CT (Fig. 7*B*), indicating that the suppression of tumor growth was mainly mediated by CD8$\alpha\beta$ CTLs rather than by NK cell cytotoxicity.

F7

AQ: M

## Discussion

In the present study we demonstrated that when OVA plus intact CT was orally administered into mice, direct OVA-specific cytotoxicity was dominantly induced in IELs rather than SCs after the first oral priming, and direct OVA-specific cytotoxicity was remarkably expanded in IELs but not in SCs after oral boosting with the same doses of OVA plus CT. Such OVA-specific CTLs were thymic conventional K$^b$ class I MHC molecule-restricted TCR$\alpha\beta^+$ CD8$\alpha\beta$ T cells (32). Moreover, the growth of the OVA-expressing tumor E.G7-OVA thymoma, established previously either in the stomach or dermis, was significantly suppressed by the oral administration of OVA plus CT. Furthermore, marked infiltration of OVA-specific TCR$\alpha\beta^+$ CD8$\alpha\beta$ CTLs with direct cytotoxicity in reduced tumor tissues was observed. These results suggest that activated CTLs with specific cytotoxicity generated at mucosal compartments by oral administration with OVA plus intact CT may be responsible for already established tumor regression.

The majority of tumor regression studies associated with activation of the immune system have focused on systemic immunity observed in the spleen, lymph nodes, and circulating blood rather than local mucosal immunity seen in gut IELs. Those studies have demonstrated only preventative results for tumor establishment by preadministration of tumor Ag plus a suitable adjuvant. In addition, to our knowledge only one study has been shown to suppress already established tumor growth by activating and expanding tumor infiltrating CD8$^+$ CTLs (23). In that study, i.v. vaccination with DCs prepulsed ex vivo with OVA-CT at day 3 and boosted at day 10 after OVA-expressing E.G7 tumor injection induced complete rejection of a visible tumor within 3 wk after the first treatment. Although the inoculation route and the materials for vaccination were different from ours, the timing of the priming and boosting to induce the suppression of already established tumor growth correlated exactly, suggesting that their methods may also initiate strong mucosal direct cytotoxicity mediated through CD8$^+$ CTLs.

Similar to our findings, they also showed that immunization with OVA-CT but not with CTB-conjugated OVA (OVA-CTB)-prepulsed DCs could successfully induce complete rejection of already established tumor growth, although OVA-CTB-prepulsed DC inoculation prevented tumor establishment but not ongoing tumor growth in the skin. Moreover, they insisted that OVA has to be coupled to CT and should be loaded onto DCs for therapeutic DC vaccination based on the observation that neither OVA-CT nor DCs pulsed with unconjugated OVA plus CT could prevent tumor progression. Nonetheless, our findings shown here apparently indicate that we were able to induce effective suppression of ongoing tumor growth by simple oral administration with unconjugated OVA and CT. These results suggest that we may control already established tumor growth at the surface compartments by activating mucosal $CD8^+$ CTLs via orally administered tumor Ag with a suitable mucosal adjuvant. Also, when OVA-CT is orally administered, the conjugation between OVA and CT may be broken through digestion by enzymes secreted in the gastrointestinal tract. Recently, we have reported that modification of OVA in the gastrointestinal tract is essential for oral tolerance induction against OVA (33). Therefore, it is possible that gastrointestinal digestion or modification of OVA may facilitate the delivery of OVA Ag into DCs, critical APCs for OVA-specific CTL induction.

For the efficient induction of such OVA-specific CTLs in vivo using DCs, Eriksson et al. have reported that OVA-CT-prepulsed DC immunization required at least two DC injections, reflecting the priming/boosting procedure (23); however, we have observed that a single oral administration of OVA plus CT seems sufficient to induce effective CTLs to prevent E.G7-OVA thymoma growth, particularly in the skin. This may be because mucosally activated CTLs through oral immunization may be more potent than systemically activated CTLs to suppress transplanted tumors at the mucosal compartment, and oral administration of OVA plus CT seems more efficient to induce mucosal CTLs than i.v. Ag-loaded DC inoculation. Further studies will be needed to explain the differences.

Although both CT-conjugated-OVA and CTB-conjugated OVA are cross-presented by MHC class I in DCs, only CT-OVA but not CTB-OVA cross-primes OVA-specific $CD8^+$ CTLs in vivo (23, 34). Additionally, DCs pulsed with intact OVA alone cannot cross-present and cross-prime CTLs (23). For the cross-priming of Ag-specific CTLs by Ag-captured immature DCs, maturation signaling via some surface molecules such as TLR-3 in those DCs is essential (35, 36). Although whole CT up-regulates the expression of MHC class II, B7.1, and B7.2 molecules on DCs in vitro, neither CTA nor CTB alone up-regulates the levels of surface markers on DCs (37, 38). Also, the binding of CTB to GM1 on DCs seems necessary to efficiently take up both CT itself and Ag and to induce cross-presentation by MHC class I molecules on DCs, whereas CTA may not be taken up to affect DCs. When DCs from GM1-lacking mice were matured in vitro, CT failed to up-regulate the expression of maturation markers and, thus, the binding of B subunits in CT to GM1 molecules on DCs is essential for the induction of DC maturation (37). It has been reported that CTA is required to not only assist in maturation but also to generate the migration of DCs (39, 40); therefore, CTB-mediated matured DCs can initiate their migration to secondary lymphoid organs and colocalization with naive T cells (38). Indeed, CT-loaded but not CTB-loaded DCs could migrate from marginal zones to T cell zones in the spleen (39) and from the subepithelial dome region to T cell zones in PPs (40); therefore, both CTA and CTB were essential for cross-priming CTLs in vivo and neither CTA nor CTB alone could induce CTLs at various compartments (Fig. 3). Taken together, although the detailed mechanisms of efficient Ag presentation via MHC class I and the maturation and migration of DCs by CT are still unknown, digested OVA might be efficiently captured by immature gut mucosal DCs in the presence of CTB and the captured Ag may be cross-presented by MHC class I during DC maturation and migration in the presence of CTA, resulting in the induction of mucosal class I MHC molecule-restricted CTLs that may cause the regression of previously established tumors.

AQ: N

AQ: O

$OVA$-specific $CD8^+$ CTLs were induced among not only the IELs but also the LPLs of the stomach, small intestine, and large intestine by oral administration of OVA plus CT, a higher percentage of OVA-specific CD8 CTLs was observed in the stomach, small intestine, and large intestine in order, and more specific CTLs were always detected among IELs than among LPLs (Fig. 4, *E* and *F*). Thus, CTLs are much easier to be induced in the upper and more superficial portions of the gastrointestinal tract when Ags are orally administrated with intact CT.

It has been reported that DCs in gastric mucosa are increased in *Helicobacter pylori* (*Hp*)-infected mice and that the response of DCs and T cells to *Hp* Ag is critical for *Hp*-induced gastritis (41). In the present study, Ag-specific CTLs in the stomach might be generated by mucosally activated DCs in the presence of CT and infiltrate-implanted gastric tumor tissues. It is possible that intestinally activated CTLs might migrate to the tumor-implanted stomach, which might also cause CTL infiltration. Actually, such effector CTLs usually express high levels of $\alpha_4\beta_7$ integrin and can home in to the gastric (42), and small and large intestinal mucosa (43) where mucosal addressin cell-adhesion molecule-1 (MadCAM-1), the ligand of $\alpha_4\beta_7$ integrin, is constitutively expressed by postcapillary endothelial cells in small (44, 45) and large intestinal lamina propria (46). Moreover, the number of gastric $\alpha_4\beta_7^{high}$ T cells increased markedly by oral administration of CT in mice (42). It has also been reported that MAdCAM-1 expression is increased in the gastric mucosa after oral administration with cholera vaccine composed of CTB and formalin-inactivated *V. cholerae* (47); therefore, MadCAM-1-expression in gastric mucosa and the recruitment of effector $\alpha 4\beta 7^{high}$ T cells to gastric mucosa might be enhanced by oral administration of the CT adjuvant and, thus, OVA-specific effector CTLs might efficiently infiltrate the OVA Ag-expressing tumor region in the stomach.

In the present study, we found that the growth of dermally implanted tumors was also suppressed by the oral administration of tumor Ag plus whole intact CT. The actual mechanisms for such suppression remains to be elucidated, but there are at least three distinct possibilities: first, the migration of Ag-specific CTLs from the gastrointestinal tract to the skin; second, the migration of Ag-presenting DCs activated in the mucosal compartments by CT; and third, the migration of both cells from the gastrointestinal tract to the skin at the same time. It has been reported that the levels of CCR4 expression, which is associated with T cell homing to the skin, are increased in gastric T cells by infection with *Hp* in humans (48). Moreover, mucosal DCs that take up Ag might migrate to regional lymph nodes near the dermal tumor and prime the CTLs there, and the CTLs could effectively infiltrate dermal tumor tissue. Indeed, Belyakov et al. demonstrated an opposite mechanism in which skin-derived DCs containing heat-labile enterotoxin of *Escherichia coli* migrated to PPs and induced mucosal CTLs by transcutaneous immunization of an Ag and CT (49). Although the detailed mechanisms of this migration of DCs between skin and mucosa are unknown, they have clearly shown that DCs can migrate between the mucosa and skin. We are currently comparing the alteration of DCs in the mucosal compartment, spleen, and lymph nodes after oral administration of an Ag plus natural CT.

Unfortunately, such natural CT is not an appropriate mucosal adjuvant for human clinical investigation (50); however, studies

using natural CT would provide important and critical information about the effect of CT that would be useful for mucosal immune activation. Based on the findings obtained by using natural CT in a mouse model system, we could establish much safer protocols with a mutant CT (51) that induces adenosine diphosphate ribosylation and cyclic adenosine monophosphate formation, which may prevent severe diarrhea as well as retain adjuvant properties. Taken together, an artificial CT-based vaccine targeting DCs may provide a strategy for efficient CTL induction and avirulent mucosal cancer vaccination.

Our data also indicate that E.G7-OVA tumor growth was suppressed by OVA-specific CTLs but not NK cells (Fig. 7*B*). Vaccination with OVA-CT-pulsed DC protects against E.G7-OVA tumor development in vivo in wild-type, NK-depleted, and CD4-deficient mice but not in CD8-deficient mice (34), indicating that the E.G7-OVA tumor might be controlled by CD8 T cells but not by NK cells or CD4 T cells. In fact, TILs in the suppressed tumor did not show any NK-related cytotoxicity (Fig. 7*B*). Moreover, it has been demonstrated that in vitro pretreatment of NK cells with CT inhibits NK cell killing of tumor (YAC-1 or P815), because G proteins in NK cell membranes are ADP ribosylated with CT and ribosylation inhibits the lysis of tumor cells (52); therefore, NK cells do not seem to be involved in the suppression of E.G7-OVA growth in vivo.

It has been shown that activated CTLs but not naive CTLs can represent antitumor (22) or antivirus (12) responses in vivo. In the present study, already established E.G7 tumor growth can be suppressed only when OVA-specific CTLs that show specific cytotoxicity without requiring in vitro restimulation are induced, particularly in the mucosal compartment. To our knowledge, this is the first demonstration of the visual suppression of already established tumor growth by the simple oral administration of tumor Ag plus mucosal adjuvant. The findings shown in the present study herald a new era for cancer immunotherapy.

## Acknowledgments

We thank Dr. Yoshihiro Kumagai and Yoshihiko Norose for useful discussions and advice.

## Disclosures

The authors have no financial conflict of interest.

## References

1. Franks, L. M., and M. A. Knowles. 2005. What is cancer? In *Introduction to the Cellular and Molecular Biology of Cancer*, 4th Ed. M. A. Knowles and P. J. Selby, eds. Oxford University Press, New York. pp. 1–24.
2. Finn, O. J. 2003. Cancer vaccines: between the idea and the reality. *Nat. Rev. Immunol.* 3: 630–641.
3. Czerkinsky, C., F. Anjuere, J. R. McGhee, A. George-Chandy, J. Holmgren, M. P. Kieny, K. Fujiyashi, J. F. Mestecky, V. Pierrefite-Carle, C. Rask, and J. B. Sun. 1999. Mucosal immunity and tolerance: relevance to vaccine development. *Immunol. Rev.* 170: 197–222.
4. Yuki, Y., and H. Kiyono. 2003. New generation of mucosal adjuvants for the induction of protective immunity. *Rev. Med. Virol.* 13: 293–310.
5. Takahashi, H. 2003. Antigen presentation in vaccine development. *Comp. Immunol. Microbiol. Infect. Dis.* 26: 309–328.
6. Hayday, A., E. Theodoridis, E. Ramsburg, and J. Shires. 2001. Intraepithelial lymphocytes: exploring the third way in immunology. *Nat. Immunol.* 2: 997–1003.
7. Offit, P. A., and K. I. Dudzik. 1989. Rotavirus-specific cytotoxic T lymphocytes appear at the intestinal mucosal surface after rotavirus infection. *J. Virol.* 63: 3507–3512.
8. Chardes, T., D. Buzoni-Gatel, A. Lepage, F. Bernard, and D. Bout. 1994. *Toxoplasma gondii* oral infection induces specific cytotoxic CD8 $\alpha\beta^+$ Thy-1$^+$ gut intraepithelial lymphocytes, lytic for parasite-infected enterocytes. *J. Immunol.* 153: 4596–4603.
9. Muller, S., M. Buhler-Jungo, and C. Mueller. 2000. Intestinal intraepithelial lymphocytes exert potent protective cytotoxic activity during an acute virus infection. *J. Immunol.* 164: 1986–1994.
10. Taunk, J., A. I. Roberts, and E. C. Ebert. 1992. Spontaneous cytotoxicity of human intraepithelial lymphocytes against epithelial cell tumors. *Gastroenterology* 102: 69–75.
11. Roberts, A. I., S. M. O'Connell, L. Biancone, R. E. Brolin, and E. C. Ebert. 1993. Spontaneous cytotoxicity of intestinal intraepithelial lymphocytes: clues to the mechanism. *Clin. Exp. Immunol.* 94: 527–532.
12. Kuribayashi, H., A. Wakabayashi, M. Shimizu, H. Kaneko, Y. Norose, Y. Nakagawa, J. Wang, Y. Kumagai, D. H. Margulies, and H. Takahashi. 2004. Resistance to viral infection by intraepithelial lymphocytes in HIV-1 P18-110-specific T-cell receptor transgenic mice. *Biochem. Biophys. Res. Commun.* 316: 356–363.
13. Takahashi, H., J. Cohen, A. Hosmalin, K. B. Cease, R. Houghten, J. L. Cornette, C. DeLisi, B. Moss, R. N. Germain, and J. A. Berzofsky. 1988. An immunodominant epitope of the human immunodeficiency virus envelope glycoprotein gp160 recognized by class I major histocompatibility complex molecule-restricted murine cytotoxic T lymphocytes. *Proc. Natl. Acad. Sci. USA* 85: 3105–3109.
14. Williams, N. A., T. R. Hirst, and T. O. Nashar. 1999. Immune modulation by the cholera-like enterotoxins: from adjuvant to therapeutic. *Immunol. Today* 20: 95–101.
15. Lencer, W. I., and B. Tsai. 2003. The intracellular voyage of cholera toxin: going retro. *Trends Biochem. Sci.* 28: 639–645.
16. Elson, C. O., and W. Ealding. 1984. Generalized systemic and mucosal immunity in mice after mucosal stimulation with cholera toxin. *J. Immunol.* 132: 2736–2741.
17. Marinaro, M., H. F. Staats, T. Hiroi, R. J. Jackson, M. Coste, P. N. Boyaka, N. Okahashi, M. Yamamoto, H. Kiyono, H. Bluethmann, et al. 1995. Mucosal adjuvant effect of cholera toxin in mice results from induction of T helper 2 (Th2) cells and IL-4. *J. Immunol.* 155: 4621–4629.
18. Bowen, J. C., S. K. Nair, R. Reddy, and B. T. Rouse. 1994. Cholera toxin acts as a potent adjuvant for the induction of cytotoxic T-lymphocyte responses with non-replicating antigens. *Immunology* 81: 338–342.
19. Carbone, F. R., and M. J. Bevan. 1989. Induction of ovalbumin-specific cytotoxic T cells by in vivo peptide immunization. *J. Exp. Med.* 169: 603–612.
20. Moore, M. W., F. R. Carbone, and M. J. Bevan. 1988. Introduction of soluble protein into the class I pathway of antigen processing and presentation. *Cell* 54: 777–785.
21. Porgador, A., H. F. Staats, B. Faiola, E. Gilboa, and T. J. Palker. 1997. Intranasal immunization with CTL epitope peptides from HIV-1 or ovalbumin and the mucosal adjuvant cholera toxin induces peptide-specific CTLs and protection against tumor development in vivo. *J. Immunol.* 158: 834–841.
22. Dalyot-Herman, N., O. F. Bathe, and T. R. Malek. 2000. Reversal of CD8$^+$ T cell ignorance and induction of anti-tumor immunity by peptide-pulsed APC. *J. Immunol.* 165: 6731–6737.
23. Eriksson, K., J. B. Sun, I. Nordstrom, M. Fredriksson, M. Lindblad, B. L. Li, and J. Holmgren. 2004. Coupling of antigen to cholera toxin for dendritic cell vaccination promotes the induction of MHC class I-restricted cytotoxic T cells and the rejection of a cognate antigen-expressing model tumor. *Eur. J. Immunol.* 34: 1272–1281.
24. Taguchi, T., J. R. McGhee, R. L. Coffman, K. W. Beagley, J. H. Eldridge, K. Takatsu, and H. Kiyono. 1990. Analysis of Th1 and Th2 cells in murine gut-associated tissues: frequencies of CD4$^+$ and CD8$^+$ T cells that secrete IFN-$\gamma$ and IL-5. *J. Immunol.* 145: 68–77.
25. Takahashi, M., E. Osono, Y. Nakagawa, J. Wang, J. A. Berzofsky, D. H. Margulies, and H. Takahashi. 2002. Rapid induction of apoptosis in CD8$^+$ HIV-1 envelope-specific murine CTLs by short exposure to antigenic peptide. *J. Immunol.* 169: 6588–6593.
26. Semple, J. W., and M. R. Szewczuk. 1986. Natural killer cells in murine muscular dystrophy: IV. Characterization of Percoll fractionated splenic and thymic natural killer cells and natural killer-sensitive thymocyte targets. *Clin. Immunol. Immunopathol.* 41: 116–129.
27. Belz, G. T., W. Xie, and P. C. Doherty. 2001. Diversity of epitope and cytokine profiles for primary and secondary influenza a virus-specific CD8$^+$ T cell responses. *J. Immunol.* 166: 4627–4633.
28. Nakatsuka, K., H. Sugiyama, Y. Nakagawa, and H. Takahashi. 1999. Purification of antigenic peptide from murine hepatoma cells recognized by class-I major histocompatibility complex molecule-restricted cytotoxic T-lymphocytes induced with B7-1-gene-transfected hepatoma cells. *J. Hepatol.* 30: 1119–1129.
29. Kilshaw, P. J., and K. C. Baker. 1988. A unique surface antigen on intraepithelial lymphocytes in the mouse. *Immunol. Lett.* 18: 149–154.
30. Russell, G. J., C. M. Parker, K. L. Cepek, D. A. Mandelbrot, A. Sood, E. Mizoguchi, E. C. Ebert, M. B. Brenner, and A. K. Bhan. 1994. Distinct structural and functional epitopes of the $\alpha$ E $\beta$ 7 integrin. *Eur. J. Immunol.* 24: 2832–2841.
31. Lefrancois, L., T. A. Barrett, W. L. Havran, and L. Puddington. 1994. Developmental expression of the $\alpha$ IEL $\beta$ 7 integrin on T cell receptor $\gamma$ $\delta$ and T cell receptor $\alpha$ $\beta$ T cells. *Eur. J. Immunol.* 24: 635–640.
32. Rocha, B., P. Vassalli, and D. Guy-Grand. 1994. Thymic and extrathymic origins of gut intraepithelial lymphocyte populations in mice. *J. Exp. Med.* 180: 681–686.
33. Wakabayashi, A., Y. Kumagai, E. Watari, M. Shimizu, M. Utsuyama, K. Hirokawa, and H. Takahashi. 2006. Importance of gastrointestinal ingestion and macromolecular antigens in the vein for oral tolerance induction. *Immunology* 119: 167–177.
34. Sun, J. B., K. Eriksson, B. L. Li, M. Lindblad, J. Azem, and J. Holmgren. 2004. Vaccination with dendritic cells pulsed in vitro with tumor antigen conjugated to cholera toxin efficiently induces specific tumoricidal CD8$^+$ cytotoxic lymphocytes dependent on cyclic AMP activation of dendritic cells. *Clin. Immunol.* 112: 35–44.

35. Fujimoto, C., Y. Nakagawa, K. Ohara, and H. Takahashi. 2004. Polyriboinosinic polyribocytidylic acid [poly(I:C)]/TLR3 signaling allows class I processing of exogenous protein and induction of HIV-specific $CD8^+$ cytotoxic T lymphocytes. *Int. Immunol.* 16: 55–63.
36. Schulz, O., S. S. Diebold, M. Chen, T. I. Naslund, M. A. Nolte, L. Alexopoulou, Y. T. Azuma, R. A. Flavell, P. Liljestrom, and C. Reis e Sousa. 2005. Toll-like receptor 3 promotes cross-priming to virus-infected cells. *Nature* 433: 887–892.
37. Kawamura, Y. I., R. Kawashima, Y. Shirai, R. Kato, T. Hamabata, M. Yamamoto, K. Furukawa, K. Fujihashi, J. R. McGhee, H. Hayashi, and T. Dohi. 2003. Cholera toxin activates dendritic cells through dependence on GM1-ganglioside which is mediated by NF-κB translocation. *Eur. J. Immunol.* 33: 3205–3212.
38. Gagliardi, M. C., F. Sallusto, M. Marinaro, A. Langenkamp, A. Lanzavecchia, and M. T. De Magistris. 2000. Cholera toxin induces maturation of human dendritic cells and licences them for Th2 priming. *Eur. J. Immunol.* 30: 2394–2403.
39. Grdic, D., L. Ekman, K. Schon, K. Lindgren, J. Mattsson, K. E. Magnusson, P. Ricciardi-Castagnoli, and N. Lycke. 2005. Splenic marginal zone dendritic cells mediate the cholera toxin adjuvant effect: dependence on the ADP-ribosyltransferase activity of the holotoxin. *J. Immunol.* 175: 5192–5202.
40. Shreedhar, V. K., B. L. Kelsall, and M. R. Neutra. 2003. Cholera toxin induces migration of dendritic cells from the subepithelial dome region to T- and B-cell areas of Peyer's patches. *Infect. Immun.* 71: 504–509.
41. Drakes, M. L., S. J. Czinn, and T. G. Blanchard. 2006. Regulation of murine dendritic cell immune responses by *Helicobacter felis* antigen. *Infect. Immun.* 74: 4624–4633.
42. Michetti, M., C. P. Kelly, J. P. Kraehenbuhl, H. Bouzourene, and P. Michetti. 2000. Gastric mucosal $\alpha_4\beta_7$-integrin-positive CD4 T lymphocytes and immune protection against *Helicobacter* infection in mice. *Gastroenterology* 119: 109–118.
43. Lefrancois, L., C. M. Parker, S. Olson, W. Muller, N. Wagner, M. P. Schon, and L. Puddington. 1999. The role of $\beta_7$ integrins in CD8 T cell trafficking during an antiviral immune response. *J. Exp. Med.* 189: 1631–1638.
44. Berlin, C., R. F. Bargatze, J. J. Campbell, U. H. von Andrian, M. C. Szabo, S. R. Hasslen, R. D. Nelson, E. L. Berg, S. L. Erlandsen, and E. C. Butcher. 1995. $\alpha_4$ integrins mediate lymphocyte attachment and rolling under physiologic flow. *Cell* 80: 413–422.
45. Berlin, C., E. L. Berg, M. J. Briskin, D. P. Andrew, P. J. Kilshaw, B. Holzmann, I. L. Weissman, A. Hamann, and E. C. Butcher. 1993. $\alpha_4\beta_7$ integrin mediates lymphocyte binding to the mucosal vascular addressin MAdCAM-1. *Cell* 74: 185–195.
46. Streeter, P. R., E. L. Berg, B. T. Rouse, R. F. Bargatze, and E. C. Butcher. 1988. A tissue-specific endothelial cell molecule involved in lymphocyte homing. *Nature* 331: 41–46.
47. Lindholm, C., A. Naylor, E. L. Johansson, and M. Quiding-Jarbrink. 2004. Mucosal vaccination increases endothelial expression of mucosal addressin cell adhesion molecule 1 in the human gastrointestinal tract. *Infect. Immun.* 72: 1004–1009.
48. Lundgren, A., C. Trollmo, A. Edebo, A. M. Svennerholm, and B. S. Lundin. 2005. *Helicobacter pylori*-specific $CD4^+$ T cells home to and accumulate in the human *Helicobacter pylori*-infected gastric mucosa. *Infect. Immun.* 73: 5612–5619.
49. Belyakov, I. M., S. A. Hammond, J. D. Ahlers, G. M. Glenn, and J. A. Berzofsky. 2004. Transcutaneous immunization induces mucosal CTLs and protective immunity by migration of primed skin dendritic cells. *J. Clin. Invest.* 113: 998–1007.
50. Clarke, L. L., B. R. Grubb, S. E. Gabriel, O. Smithies, B. H. Koller, and R. C. Boucher. 1992. Defective epithelial chloride transport in a gene-targeted mouse model of cystic fibrosis. *Science* 257: 1125–1128.
51. Yamamoto, S., Y. Takeda, M. Yamamoto, H. Kurazono, K. Imaoka, M. Yamamoto, K. Fujihashi, M. Noda, H. Kiyono, and J. R. McGhee. 1997. Mutants in the ADP-ribosyltransferase cleft of cholera toxin lack diarrheagenicity but retain adjuvanticity. *J. Exp. Med.* 185: 1203–1210.
52. Maghazachi, A. A., A. Al-Aoukaty, C. Naper, K. M. Torgersen, and B. Rolstad. 1996. Preferential involvement of Go and Gz proteins in mediating rat natural killer cell lysis of allogeneic and tumor target cells. *J. Immunol.* 157: 5308–5314.

# Prospects for the Therapeutic Application of Lentivirus-Based Gene Therapy to HIV-1 Infection

Takuya Yamamoto[1,2] and Yasuko Tsunetsugu-Yokota[1,*]

[1]*Department of Immunology, National Institute of Infectious Diseases, Toyama 1-23-1, Shinjuku-ku, Tokyo 162-8640, Japan;* [2]*Division of Cellular and Molecular Biology, Department of Cancer Biology, The Institute of Medical Science, The University of Tokyo, 4-6-1 Shirokane-dai, Minato-ku, Tokyo 108-8639, Japan*

**Abstract:** Highly active antiretroviral therapy is not sufficient to fully control HIV replication and problems of side effects and escape mutation have emerged. Current prophylactic and therapeutic vaccine strategies appear to be unable to confer full protection. However, given the rapid recent progress made in RNA interference and lentivirus technologies, it may soon be possible to develop effective gene therapies against HIV infection. We describe here the recent progress made in the lentivirus-based HIV-1-targeting RNAi system and the possibility that this system can be used to generate an anti-HIV-1 gene therapy. We speculate that this system would be most useful if it would be used in a coordinated manner with vaccines that can initiate and maintain potent anti-HIV immunity.

**Keywords:** RNAi, lentivirus vector, gene therapy, HIV infection, vaccines.

## INTRODUCTION

Over the last few years, the rapid increase in the rate of human immunodeficiency virus (HIV) infection in many areas of the world has been a major focus of the international discourse about global health care issues. UNAIDS estimates that over 10000 people are newly infected every day, with the total number of HIV-infected individuals now reaching approximately 40 million (http://www.unaids.org/en/).

The development of highly active anti-retroviral therapy (HAART), a combination chemotherapy involving a protease inhibitor and reverse transcriptase inhibitors, allowed us to control HIV-1 replication almost completely, and the death toll from AIDS decreased dramatically. However, our initial enthusiasm was dampened when it was realized that HAART does not eradicate the virus, which latently persists for life in resting memory $CD4^+$ T cells [1]. On the other hand, HIV-1-infected patients treated with HAART have a broad spectrum of clinical outcomes; while most patients with an undetectable viral load also evince elevated blood CD4 counts, some show poor $CD4^+$ T-cell recovery despite having undetectable plasma virus loads [2]. Furthermore, on the contrary to the initial hopeful predictions that HAART would lead to immune system recovery [3, 4], multiple clinical cohort studies revealed that even though HAART reduces the viral load to undetectable levels, this is not necessarily followed by full recovery of the immune functions that are depressed by the virus. Instead, it appears that the immune system in HIV patients remains injured and is therefore often unable to mount adequate anti-HIV immune responses, which is why the virus frequently rebounds upon HAART discontinuation [5]. Therefore, these observations suggest that effective treatment of chronic HIV infection will require the full recovery of the immune functions that are depressed by the virus and are needed to control viral replication. Currently, diverse therapeutic vaccine regimens have been designed to stimulate anti-HIV immunity in chronically HIV-infected individuals with the aim of reducing the viral rebound upon discontinuation of HAART [6]. These studies are still ongoing and their outcomes are as yet unclear.

The provision of antiviral drugs to populations suffering from the AIDS pandemic is faced with considerable economic and logistic difficulties because these populations are generally in resource-poor countries. This makes a compelling case for the development of a safe, effective and inexpensive prophylactic vaccine. Accumulating evidence suggests that traditional vaccine strategies will not confer protection against HIV-1. Currently, it is hoped that newly developed vaccines, for example, DNA prime and recombinant adenovirus boost immunization strategies, may provide more effective immunity [7]. Numerous trials testing such preventative AIDS vaccine are currently underway (http://www.iavireport.org/trialsdb/). However, it should be noted that a common barrier to the development of an ideal vaccine is that we still do not fully understand the nature of the protective immunity that can prevent HIV-1 infection.

Two technologies that may be very useful in developing anti-HIV-1 therapies and prophylactic vaccines include RNA interference (RNAi) and lentivirus (LV) delivery systems. RNAi is the most ubiquitously occurring endogenous gene regulatory mechanism as it is found in a diverse group of organisms that includes plants, invertebrates and mammalian cells [8]. RNAi is mediated by double-stranded RNAs (dsRNAs) or short-hairpin RNAs (shRNAs) that are less than 30 nucleotides long. These molecules are known as small interfering RNA (siRNA) and they can potently and specifically trigger gene silencing by inducing the degradation of target messenger RNA in a sequence-specific manner. Such

*Address correspondence to this author at the Department of Immunology, National Institute of Infectious Diseases, Toyama 1-23-1, Shinjuku-ku, Tokyo 162-8640, Japan; Tel: +81 3 5285 1111; Fax: +81 3 5285 1150; E-mail: yyokota@nih.go.jp

1566-5232/08 $55.00+.00 

gene-specific inhibition may be useful for treating a variety of human genetic and infectious diseases, including HIV-1 [9, 10]. To deliver siRNA into target cells or tissues, viral and non-viral gene delivery systems have been developed. In particular, LV vectors are very useful, as they can be targeted to a wide variety of cells and tissues. Many reviews have described the potential of LV-mediated RNAi gene therapy for preventing HIV-1 replication and thereby controlling HIV-1 infections [11-14]. However, numerous clinical studies of chronic HIV patients on HAART indicate that AIDS cannot be cured by simply controlling viral replication [2]. We believe that long-term control of HIV-1 will require that treatments inhibiting HIV replication are administered in a coordinated manner with measures aiming to induce and prolong anti-HIV immunity. With this in mind, we will here review and discuss the development of AIDS vaccines and the potential of RNAi-based gene therapy using LV vectors as a novel vaccine strategy.

## 1. VACCINE STRATEGIES FOR HIV: WHICH IMMUNE RESPONSES ARE PROTECTIVE AGAINST HIV?

The genomes of HIV and simian immunodeficiency virus (SIV) contain structural (*gag, pol,* and *envelope*), regulatory (*rev* and *tat*), and accessory (*nef, vif, vpr* [or *vpx*] and *vpu*) genes (Fig. **1a**). Of these, the *envelope (env)* gene is of particular significance since it is believed to be a major target of neutralizing host immune responses. The *env* gene product is cleaved into two components, namely, the trimeric, surface gp120 protein and transmembrane gp41. The prototype HIV vaccines employed recombinant gp120 (rgp120) to elicit neutralizing antibodies but were not protective, as shown by several large scale human clinical trials [15]. It was then shown that the antibodies elicited by rgp120 fail to neutralize HIV-1 isolates circulating in the blood of infected individuals [16]. However, it was recently revealed that anti-Envelope neutralizing antibodies may help limit HIV replication [17]. Thus, it may still be desirable to attempt to generate neutralizing antibodies by vaccination. An additional impediment to this goal is the possibility of inducing an unwanted autoimmune response. This possibility was suggested by the observation that the two broadly neutralizing mAbs 2F5 and 4E10 cross-react with the autoantigen phospholipid cardiolipin [18]. Nevertheless, the safe elicitation of neutralizing antibodies with broad specificity continues to be the subject of considerable effort in the field.

It has been suggested that $CD8^+$ cytotoxic T cells (CTLs) are responsible for the rapid virus reduction that occurs after viral titers peak [19, 20]. The importance of CTLs in controlling both acute and chronic SIV infections was then revealed by depleting CD8 cells in a SIV model [21]. These observations led to a shift in HIV-1 vaccine research efforts towards the development of a recombinant HIV protein-expressing DNA or virus that potently induces HIV-specific CTLs. For this purpose, plasmid DNA and recombinant viruses (including vaccinia, adeno, and sendai virus) have been utilized. The target of most CTL-based vaccines is the gag protein (see http://www.iavireport.org/trialsdb/). These vaccines involve a priming injection with DNA followed by a boost with a protein or a viral vector (prime-boost regimen). Among them, the CTL-based vaccine utilizing a SIV- DNA prime/Sendai virus vector boost conferred the best protection in rhesus macaques challenged with SIVmac239, which causes chronic persistent infection in these animals [22]. Such successful SIV vaccine models may help us to understand which host responses are protective against HIV-1.

## 2. TARGETING HIV-1 BY RNAI TECHNOLOGY

HAART is not a failsafe measure that can rescue people from AIDS, even in industrial countries. The prolonged usage of antiretroviral drugs can cause serious side effects and accelerate the emergence of drug-resistant HIV mutants. Consequently, the development of novel antiretroviral drugs continues to be an important objective. An new approach became available when the RNAi system was first described

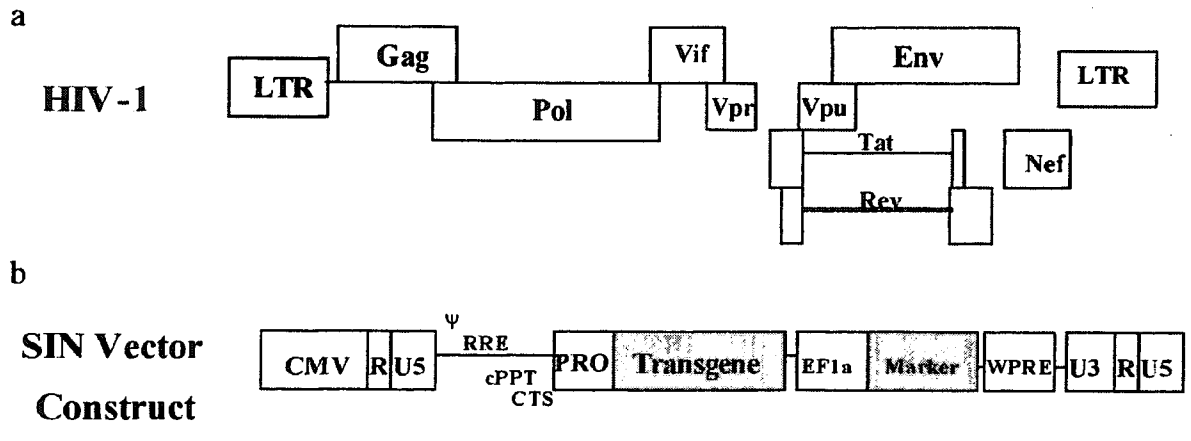


**Fig. (1).** Genome organization of HIV-1 and lentivirus vector. (a) The locations of the ORFs (boxes) indicate the reading frames of the deduced proteins. (b) HIV vector construct structures. The self-inactivating (SIN) is shown. The U3 region of the 5' long terminal repeat (LTR) in the vector constructs was replaced with the cytomegalovirus (CMV) promoter, resulting in Tat-independent transcription in conjunction with high levels of expression. The SIN vector was constructed by deleting 133 bp in the U3 region of the 3' LTR, including the TATA box and binding sites for the transcription factors Sp1 and NF-kappaB.

in mammalian cells. RNAi induces the post-transcriptional silencing of a specific gene. It was then shown that by programming the host to produce siRNA duplexes that correspond to different viral sequences, an effective antiviral response can be raised. For example, Novina *et al.* showed that when H9 T cell lines are transfected with 21-nt dsRNAs corresponding to CD4 and *gag* (p24) genes, these cells become resistant to HIV-1 (NL43 and BAL) infection [Novina *et al.*, 2002]. Similarly, Song *et al.* showed that transfection of primary macrophages with synthetic siRNAs corresponding to CCR5 and *gag* (p24) genes inhibited HIV replication in these cells [Song *et al.*, 2003]. Other groups have also demonstrated that the RNAi induced by introducing HIV-specific siRNAs can transiently inhibit HIV replication in T-cells [23-27]. This revolutionary finding in functional genomics suggested that RNAi-based therapies may be designed to block not only HIV infection [13] but also other virus infections in humans, including respiratory syncytial virus (RSV), Hepatitis C virus (HCV), and pandemic influenza [9, 10].

While many RNAi studies have employed transfection with synthetic siRNAs, shRNAs can also be utilized for gene silencing. To do this, the shRNA encoded by DNA is introduced into the cell nucleus by viral and non-viral vector systems. The shRNA is produced by both sense and antisense strands. Upon transcription, it forms a hairpin ranging from 6 to 12 nucleotides that activates the endogenous RNAi system (Fig. 2). Expressed shRNAs have an advantage over synthetic siRNA transfection in that they are able to mediate the long-term, stable knockdown of their target tanscripts [10]. An example of the use of shRNA for producing antiviral RNAi is our Nef366 shRNA expression system, which is driven by Pol III promoter and targets HIV Nef366 (this is the *nef* gene sequence that overlaps the 3 LTR U3) [28]. We showed that the expression of shRNA against Nef366 (shNef366) by monocytic cell lines strongly inhibits the replication of HIV-1 at an early stage of HIV infection. Since the U3 region is required during reverse transcription for the first template transfer and integration of the viral genome into the host genome, we believe that the siRNA targeting the U3 region induced not only the specific degradation of *nef* mRNA but also inhibited HIV-1 reverse transcription. Significantly, escape mutants were not observed in the primary macrophage culture during the 3 weeks of observation, even though others have observed escape mutations in RNAi experiments targeting *nef* or *tat* [29, 30]. This reflects that fact that the nef/U3 sequence we targeted is highly conserved and is thus likely to be more resistant to mutation. Recently, Sabariegos *et al.* studied HIV-1 RNAi escape mutations extensively and demonstrated that optimal HIV-1 gene silencing requires complete homology within most of the target sequence and that substitutions at only a few positions at the 5' and 3' ends are partially tolerated [31]. Thus, to avoid the emergence of escape mutations, it may be necessary to employ multiple shRNAs that target different conserved sites in HIV or host-derived factors that contribute to viral replication [13].

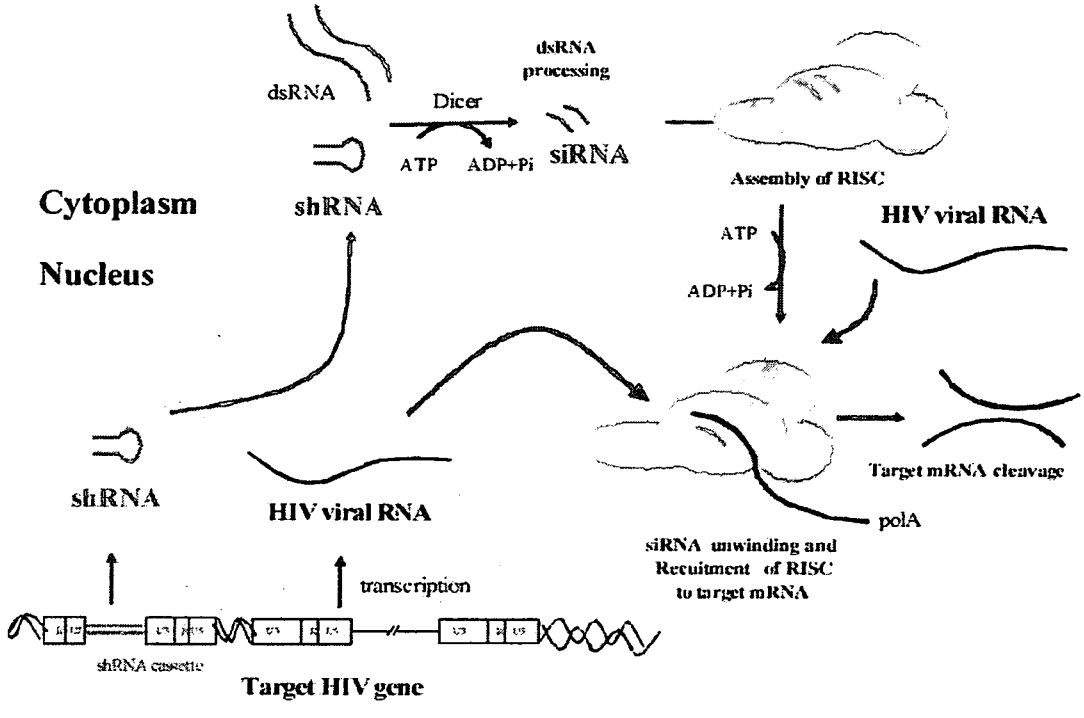


**Fig. (2).** RNAi mechanisms. RNAi is initiated by the Dicer enzyme, which processes double-stranded RNAs (dsRNAs) or short-hairpin RNAs (shRNAs) into ~22-nucleotide small interfering RNAs (siRNAs). The siRNAs are incorporated into a multicomponent nuclease called the RNA-induced silencing complex (RISC). Recent reports suggest that RISC must be activated from a latent form that contains a double-stranded siRNA into the active RISC form; this is accomplished by the unwinding of the siRNA [59]. RISC then uses the unwound siRNA to guide its substrate selection. This leads to the near-perfect formation of complementary mRNA and results in mRNA destruction.

## 3. SELECTION OF VIRAL VECTORS FOR EFFICIENT GENE DELIVERY

How to deliver siRNA into specific tissues or cells is a critical issue for gene therapy. Both viral and non-viral delivery systems have been developed for this purpose [10]. However, viral delivery systems that permit the expression of shRNA would be more suitable for chronic disease, which requires that RNAi operates continuously over a prolonged period. The virus vectors that are currently being utilized for gene therapy include adenovirus (AdV), adeno-associated virus (AAV), and LV. The advantageous and disadvantageous characteristics of these viral vectors are summarized in Table 1. AdV type 5 was first used clinically for human gene therapy of cystic fibrosis patients in 1993 [32]. Since then, the AdV vector system has been greatly improved and is now widely utilized in gene transfer both *in vitro* and *in vivo* (review in [33]). However, the transience of the transgene expression and preexisting immunity against AdV make the AdV vector less favorable as a vector for delivering shRNA into humans. The AAV vector system was also developed for gene therapy [34-36]. AAV is a small non-pathogenic virus with a wide organ/tissue tropism that has a single strand 4.7 kb DNA genome. Although the packaging capacity of the AAV vector is very small, it has the advantage that it can transduce a gene into non-dividing cells and may therefore maintain gene expression for a relatively long time. However, because the currently available AAV vectors do not contain their own machinery to carry out site-specific integration, their transgene expression is still transient. Furthermore, as with the AdV vector, preexisting immunity against AAV affects the efficacy of gene transduction with this vector. Moreover, the immune response against AAV-infected target cells may greatly reduce transgene expression, as was demonstrated recently in a clinical application of a AAV-based gene delivery system [37].

A replication-defective LV vector derived from the HIV-1 genome was developed almost a decade ago and has since then undergone significant improvements in terms of its safety and efficiency for use in gene therapy [14, 38]. It offers the advantages of long-term expression, cell- and tissue-specific tropism, and a large packaging capacity that can deliver therapeutic genes. Unlike other retroviruses, LV vectors do not necessarily require cell division for proviral integration. Indeed, it has been shown that this vector can transduce primary resting hematopoietic cells and neuronal cells *in vitro*. In addition, LV vectors are sufficiently robust for *in vivo* administration. LV-based technology does carry the risk of inducing insertional mutagenesis; this risk is common to gene therapy involving retrovirus vectors and is a significant cause for concern. Heightening this concern is that patients with X-linked severe combined immunodeficiency (SCID) who were given Moloney Murine Leukemia Virus (MuLV)-based gene therapy suffered a serious adverse effect due to the selective integration of MuLV near the LMO2 locus [39]. However, adenosine deaminase deficiency-SCID patients did not show evidence of insertional mutagenesis when they were treated with retrovirus (MuLV) gene transfer [40]. Notably, an extensive search for the integration sites of MuLV and HIV-1 has revealed that whereas MuLV preferentially targets transcription start or promoter regions, HIV-1 integration favors genes that are actively transcribed [41-43]. This suggests that the risks of insertional mutagenesis may depend on the vector system used, the cells being targeted, and the genomic site in which the transgene is expressed. HIV-based LV vectors that integrate randomly across the entire transcribed region may be less likely to trigger insertional mutagenesis than MuLV-based retrovirus vectors. An attempt has been made to make LV vectors safer by producing a third-generation LV vector entitled self inactivation (SIN) vector. In this vector, the viral 3 LTR U3 region was deleted along with the packaging signal and unnecessary accessory genes (*tat, nef, vpr, vpu and vif*) (Fig. **1b**) [44, 45]. This SIN vector is expected to improve the safety of LV-based gene therapy because the viral LTR enhancer/promoter activity in the U3 region is eliminated. However, it would be desirable to develop even safer LV vectors in which the genome site where integration occurs can be easily manipulated. Such directed integration to specific target sites has been achieved by one group by using viral integrase fused with a sequence-specific DNA-binding protein [46, 47]. Moreover, eliminating the integration capability of LV vectors has also been shown recently to not seriously affect the *in vitro* and *in vivo* gene transfer and expression efficiency of this system [48, 49].

The great advantage of using the LV vector is that it is possible to target the vector to specific tissues or cells by

**Table 1. Virus Vectors Used for Gene Therapy**

| Delivery system | Lentivirus | Adenovirus (type5) | AAV (type2) |
|---|---|---|---|
| Infects dividing cells | + | + | + |
| Infects non-dividing cells | + | +/- | + |
| Long-term expression | + | - | + |
| Host cell integration | + (random) | - | + (specific; AAVS1) |
| Max. Insert Size | ~10 kb | 7~9 kb | 3~5 kb |
| Host immunogenicity | - | High | Low |
| Receptor | independent | CAR | $\alpha_v\beta_5$, heparan sulfate proteoglycan, c-Met, FGFR |

modifying the virion envelope [14]. Retrovirus and LV vectors are remarkably compatible with a broad range of viral envelope glycoprotein. The replacement of the native retrovirus/LV envelope with a helper plasmid that expresses heterologous envelope glycoproteins is called pseudotyping. Retrovirus/LV pseudotyping generally involves the stable vesicular stomatitis virus glycoprotein (VSV-G), which has a broad cell tropism. However, because VSV-G is sometimes cytotoxic, pseudotyping with envelopes from amphotropic viruses or feline endogenous retrovirus has also been used to produce an efficient gene delivery system for hematopoietic stem cells [50, 51]. Furthermore, it is sometimes necessary to target LV vector to a particular cell type. To do so, other envelopes are used. For example, since VSV pseudotype vectors are inefficient with airway epithelial cells, pseudotyping with envelopes from the Ebola virus or Jaagsiekte Sheep Retrovirus has been used to deliver the gene to the lung[52, 53]. Moreover, Yang *et. al.* have developed a novel method to target LV vector to a desired cell type by incorporating an antibody and a fusogenic protein into the LV surface [54]. The antibody recognizes a specific surface antigen of the target cells while the fusogen, which is derived from a virus envelope, triggers pH-dependent fusion of the vector with the target cell membrane. When CD20 was used as a model antigen, this technique was successful in selectively transducing GFP into B cells both *in vitro* and *in vivo* [54]. This result greatly enhances the potential of LV in gene therapy and suggests that gene therapy could be carried out by a procedure as simple as intravenous injection.

## 4. POTENTIAL USE OF THE LV-BASED SHRNA EXPRESSION SYSTEM AS A NOVEL AIDS VACCINE

Several groups have demonstrated that HIV replication can be inhibited when siRNA duplexes that are specific for the HIV genome or HIV replication intermediate RNA are introduced by a LV or retrovirus vector system [11, 13]. For example, Das *et al.* showed that T-cell lines containing a murine retrovirus vector expressing Nef-specific siRNAs inhibited HIV-1 replication in a stable manner [30]. However, the virus replication block did not last long as escape mutants emerged rapidly. However, as described above, when we used our LV expression system to induce primary monocyte-derived macrophages to stably express shNef366, HIV-1 replication in these cells was abrogated for at least 3 weeks and the emergence of escape viruses was not detected [28]. Significantly, this system also substantially reduced HIV-1 infectivity.

To effectively treat a chronic HIV infection, it is necessary that the immune system is healthy enough to suppress HIV viremia, thereby forcing the clinical latency of the virus. It has been shown by an early study that strong proliferative HIV-specific $CD4^+$ T cell-responses are associated with the control of viremia by individuals who suppress viremia in the absence of antiviral therapy [5]. However, in chronic HIV-1 infection with uncontrolled viremia, HIV-specific $CD4^+$ T cells are functionally impaired [55][56]. In particular, $CD4^+$ T-cell proliferation is severely stunted; this inverse relationship between high plasma viral load and $CD4^+$ T-cell proliferation has been well documented[5]. Significantly, it appears that this functional impairment is sustained even when viremia has been controlled by antiviral therapy, and that this prevents the patient from controlling the infection upon HAART discontinuation. For example, Jansen *et al.* recently showed that although patients with acute HIV-1 infection who are treated with HAART early after infection have higher HIV-specific IFN-γ and IL-2-producing $CD4^+$ T-cell numbers than late-treated patients, they were no more capable of controlling their infection [57]. This was attributed to the fact that the $CD4^+$ T-cell proliferative capacities of both groups were equally low. Thus, HAART does not preserve the virus-controlling immune functions of $CD4^+$ T cells, regardless when after infection it is administered.

Why HIV-specific $CD4^+$ T-cell proliferation remains impaired despite HAART-induced control over viremia remains unclear. We speculate that it may be because during latency, HIV-1 resides in resting memory T cells [1], particularly in HIV-specific memory $CD4^+$ T cells [58]. Upon vaccination aiming to activate and expand HIV-specific $CD4^+$ T cells or renewed viremia, a situation in which a desired outcome is impossible to attain occurs: the activation of these cells provokes HIV-1 replicative activity within them, which in turn prevents them from proliferating and mounting a major attack on the virus. Supporting this notion is that we recently found that the proliferative capacity of HIV-specific $CD4^+$ T cells can be restored by inhibiting HIV-1 replication using our Lenti shNef366 system (Yamamoto *et al.* manuscript in preparation). Our observation also points to a novel prophylactic as well as therapeutic approach to HIV-1 infection, namely, the use of LV-mediated RNAi in combination with immunostimulatory vaccines. We propose that the RNAi-mediated block on ongoing HIV-1 replication in $CD4^+$ T cells might help these cells proliferate in response to Gag-specific immunostimulatory vaccines. Under the umbrella of continuing RNAi-mediated obstruction of virus replication, these cells would then be able to effectively control residual viremia. This approach would require an LV vector system that targets $CD4^+$ T cells. Such targeting of a particular cell type in gene therapy seems quite feasible [54]. Thus, further gene therapy-related modifications of the LV system may help to produce a treatment regimen that could assist in slowing or even halting the currently uncontrollable expansion of HIV infection.

## 5. CONCLUSIONS AND FUTURE PROSPECTS

The identification of RNAi and the fact that it can be harnessed to mount an antiviral response have greatly increased our options in the fight against HIV-1. It is likely that anti-HIV shRNA-expressing LV vectors will soon be tested in the clinic as a potential gene therapy [10]. However, it remains unclear how effective this approach will be and whether it could be employed routinely for preventing HIV infections and for treating clinical symptoms or disease progression associated with HIV infection.

The new LV-based AIDS vaccine concept that we discussed in the preceding section is depicted schematically in Fig. **3**. Fig. **3a** shows the situation with current vaccination strategies, which generally aim only to induce anti-HIV immune responses. Given that HIV selectively infects HIV-specific $CD4^+$ memory T cells and is stimulated to replicate when these cells are activated, which in turn prevents these

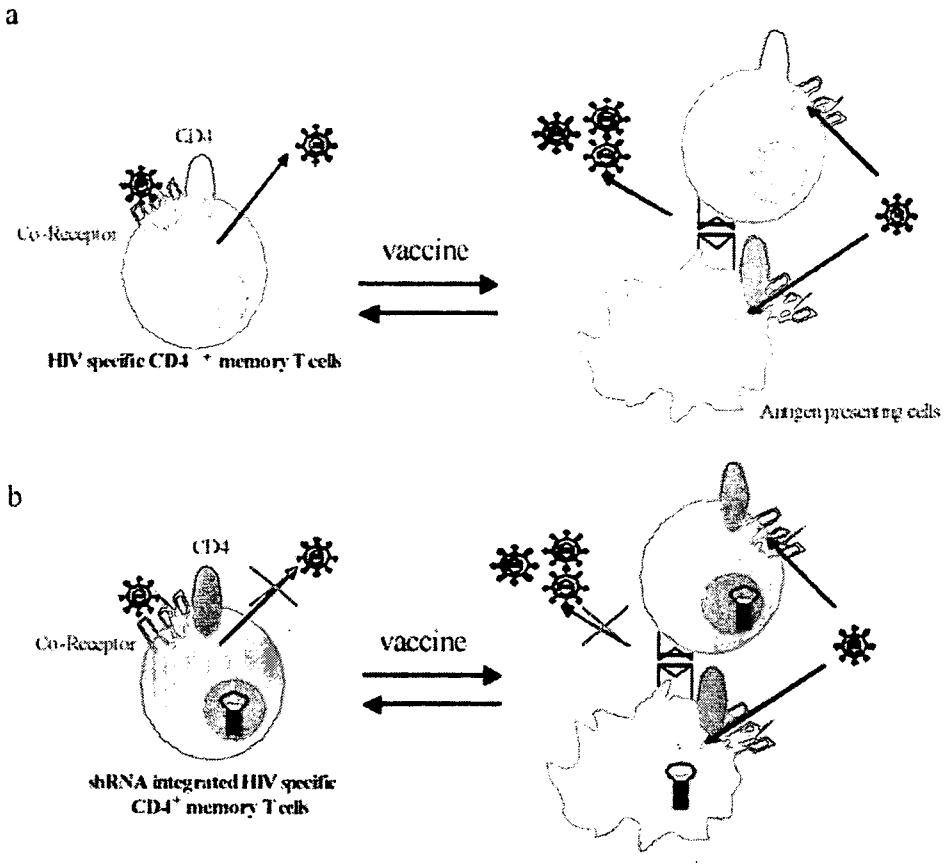


**Fig. (3).** Our model of RNAi-based gene therapy against HIV. (a) Current AIDS vaccine strategies. (b) Our proposed AIDS vaccine strategy, which is based on lentivirus vector-mediated RNAi gene therapy. After shRNA is integrated into the genome of CD4+ T cells, an immunostimulatory AIDS vaccine is administered. The symbol in the nuclei shows shRNA.

cells from proliferating, it is possible that these strategies may actually worsen the situation, as they induce an ineffective immune response while simultaneously enhancing virus production; moreover, the vaccine increases the frequency of intimate cell to cell contact between HIV-specific helper $CD4^+$ T cells and latently infected antigen-presenting cells such as macrophages and dendritic cells contact, thereby promoting virus dissemination (Fig. **3a**). Our concept differs from most other HIV vaccine development strategies in that it seeks to induce strong HIV-specific immune responses while simultaneously blocking the HIV-1 replicative activity that is provoked upon host T-cell activation (Fig. **3b**). This has several major advantages in that it on the one hand promotes the efficacy of the immunostimulatory vaccine while on the other preventing further virus production and infection of newly generated T cells and antigen-presenting cells. The efficacy of this concept may be further enhanced by expanding the range of host cells that are transduced *via* LV with HIV shRNA to include antigen-presenting cells as well as HIV-specific $CD4^+$ T cells. We speculate that this concept may also be suitable for prophylactic use.

In conclusion, an LV gene therapy-based AIDS vaccine that specifically inhibits viral replication may, when used in a coordinated fashion with immunostimulatory vaccines, promote their efficacy. Such a strategy, when applied therapeutically and perhaps also prophylactically, may help control or even eradicate HIV.

## ACKNOWLEDGEMENTS

This paper is partly based on our collaborative study with Prof. Brigitte Autran (Laboratory of Cellular Immunology, Pitié-Salétrière Hospital, Paris, France). We thank her, her laboratory staff, and those of our Department of Immunology, NIID, for their kind help and valuable discussions. This paper was supported by grants from the Ministry of Health, Labor and Welfare of Japan and from the Health Science Foundation of Japan.

## REFERENCES

[1] Pierson T, McArthur J, Siliciano RF. Reservoirs for HIV-1: mechanisms for viral persistence in the presence of antiviral immune responses and antiretroviral therapy. Annu Rev Immunol 18: 665-708 (2000).

[2] Aiuti F, Mezzaroma I. Failure to reconstitute CD4+ T-cells despite suppression of HIV replication under HAART. AIDS Rev 8 2: 88-97 (2006).

[3] Autran B, Carcelain G, Li TS, *et al.* Positive effects of combined antiretroviral therapy on CD4+ T cell homeostasis and function in advanced HIV disease. Science 277 5322: 112-6 (1997).

[4] Li TS, Tubiana R, Katlama C, *et al.* Long-lasting recovery in CD4 T-cell function and viral-load reduction after highly active antiret-

roviral therapy in advanced HIV-1 disease. Lancet 351 9117: 1682-6 (1998).
[5] Rosenberg ES, Billingsley JM, Caliendo AM, *et al.* Vigorous HIV-1-specific CD4+ T cell responses associated with control of viremia. Science 278 5342: 1447-50 (1997).
[6] Autran B, Carcelain G, Combadiere B, Debre P. Therapeutic vaccines for chronic infections. Science 305 5681: 205-8 (2004).
[7] Letvin NL. Progress and obstacles in the development of an AIDS vaccine. Nat Rev Immunol 6 12: 930-9 (2006).
[8] Elbashir SM, Harborth J, Lendeckel W, *et al.* Duplexes of 21-nucleotide RNAs mediate RNA interference in cultured mammalian cells targeted mRNA degradation by double-stranded RNA *in vitro*. Nature 411 6836: 494-8 (2001).
[9] Bumcrot D, Manoharan M, Koteliansky V, Sah DW. RNAi therapeutics: a potential new class of pharmaceutical drugs. Nat Chem Biol 2 12: 711-9 (2006).
[10] Kim DH, Rossi JJ. Strategies for silencing human disease using RNA interference. Nat Rev Genet 8 3: 173-84 (2007).
[11] Morris KV, Rossi JJ. Lentivirus-mediated RNA interference therapy for human immunodeficiency virus type 1 infection. Hum Gene Ther 17 5: 479-86 (2006).
[12] Nekhai S, Jerebtsova M. Therapies for HIV with RNAi. Curr Opin Mol Ther 8 1: 52-61 (2006).
[13] Scherer L, Rossi JJ, Weinberg MS. Progress and prospects: RNA-based therapies for treatment of HIV infection. Gene Ther 14 14: 1057-64 (2007).
[14] Wiznerowicz M, Trono D. Harnessing HIV for therapy, basic research and biotechnology. Trends Biotechnol 23 1: 42-7 (2005).
[15] Cohen J. Public health. AIDS vaccine trial produces disappointment and confusion. Science 299 5611: 1290-1 (2003).
[16] Graham BS, Mascola JR. Lessons from failure--preparing for future HIV-1 vaccine efficacy trials. J Infect Dis 191 5: 647-9 (2005).
[17] Humbert M, Dietrich U. The role of neutralizing antibodies in HIV infection. AIDS Rev 8 2: 51-9 (2006).
[18] Haynes BF, Fleming J, St Clair EW, *et al.* Cardiolipin polyspecific autoreactivity in two broadly neutralizing HIV-1 antibodies. Science 308 5730: 1906-8 (2005).
[19] Borrow P, Lewicki H, Hahn BH, Shaw GM, Oldstone MB. Virus-specific CD8+ cytotoxic T-lymphocyte activity associated with control of viremia in primary human immunodeficiency virus type 1 infection. J Virol 68 9: 6103-10 (1994).
[20] Koup RA, Safrit JT, Cao Y, *et al.* Temporal association of cellular immune responses with the initial control of viremia in primary human immunodeficiency virus type 1 syndrome. J Virol 68 7: 4650-5 (1994).
[21] Schmitz JE, Kuroda MJ, Santra S, *et al.* Control of viremia in simian immunodeficiency virus infection by CD8+ lymphocytes. Science 283 5403: 857-60 (1999).
[22] Matano T, Kobayashi M, Igarashi H, *et al.* Cytotoxic T lymphocyte-based control of simian immunodeficiency virus replication in a preclinical AIDS vaccine trial. J Exp Med 199 12: 1709-18 (2004).
[23] Capodici J, Kariko K, Weissman D. Inhibition of HIV-1 infection by small interfering RNA-mediated RNA interference. J Immunol 169 9: 5196-201 (2002).
[24] Dave RS, Pomerantz RJ. Antiviral effects of human immunodeficiency virus type 1-specific small interfering RNAs against targets conserved in select neurotropic viral strains. J Virol 78 24: 13687-96 (2004).
[25] Jacque JM, Triques K, Stevenson M. Modulation of HIV-1 replication by RNA interference. Nature 418 6896: 435-8 (2002).
[26] Novina CD, Murray MF, Dykxhoorn DM, *et al.* siRNA-directed inhibition of HIV-1 infection. Nat Med 8 7: 681-6 (2002).
[27] Song E, Lee SK, Dykxhoorn DM, *et al.* Sustained small interfering RNA-mediated human immunodeficiency virus type 1 inhibition in primary macrophages. J Virol 77 13: 7174-81 (2003).
[28] Yamamoto T, Miyoshi H, Yamamoto N, *et al.* Lentivirus vectors expressing short hairpin RNAs against the U3-overlapping region of HIV nef inhibit HIV replication and infectivity in primary macrophages. Blood 108 10: 3305-12 (2006).
[29] Boden D, Pusch O, Lee F, Tucker L, Ramratnam B. Human immunodeficiency virus type 1 escape from RNA interference. J Virol 77 21: 11531-5 (2003).
[30] Das AT, Brummelkamp TR, Westerhout EM, *et al.* Human immunodeficiency virus type 1 escapes from RNA interference-mediated inhibition. J Virol 78 5: 2601-5 (2004).
[31] Sabariegos R, Gimenez-Barcons M, Tapia N, Clotet B, Martinez MA. Sequence homology required by human immunodeficiency virus type 1 to escape from short interfering RNAs. J Virol 80 2: 571-7 (2006).
[32] Engelhardt JF, Yang Y, Stratford-Perricaudet LD, *et al.* Direct gene transfer of human CFTR into human bronchial epithelia of xenografts with E1-deleted adenoviruses. Nat Genet 4 1: 27-34 (1993).
[33] Campos SK, Barry MA. Current advances and future challenges in Adenoviral vector biology and targeting. Curr Gene Ther 7 3: 189-204 (2007).
[34] Gao G, Vandenberghe LH, Wilson JM. New recombinant serotypes of AAV vectors. Curr Gene Ther 5 3: 285-97 (2005).
[35] Mizukami H, Ozawa K. [Utility of AAV vectors derived from novel serotypes]. Yakugaku Zasshi 126 11: 1021-8 (2006).
[36] Vasileva A, Jessberger R. Precise hit: adeno-associated virus in gene targeting. Nat Rev Microbiol 3 11: 837-47 (2005).
[37] Manno CS, Pierce GF, Arruda VR, *et al.* Successful transduction of liver in hemophilia by AAV-Factor IX and limitations imposed by the host immune response. Nat Med 12 3: 342-7 (2006).
[38] Sinn PL, Sauter SL, McCray PB, Jr. Gene therapy progress and prospects: development of improved lentiviral and retroviral vectors--design, biosafety, and production. Gene Ther 12 14: 1089-98 (2005).
[39] Hacein-Bey-Abina S, Von Kalle C, Schmidt M, *et al.* LMO2-associated clonal T cell proliferation in two patients after gene therapy for SCID-X1. Science 302 5644: 415-9 (2003).
[40] Aiuti A, Slavin S, Aker M, *et al.* Correction of ADA-SCID by stem cell gene therapy combined with nonmyeloablative conditioning. Science 296 5577: 2410-3 (2002).
[41] De Palma M, Montini E, Santoni de Sio FR, *et al.* Promoter trapping reveals significant differences in integration site selection between MLV and HIV vectors in primary hematopoietic cells. Blood 105 6: 2307-15 (2005).
[42] Schroder AR, Shinn P, Chen H, *et al.* HIV-1 integration in the human genome favors active genes and local hotspots. Cell 110 4: 521-9 (2002).
[43] Wu X, Li Y, Crise B, Burgess SM. Transcription start regions in the human genome are favored targets for MLV integration. Science 300 5626: 1749-51 (2003).
[44] Bai Y, Soda Y, Izawa K, *et al.* Effective transduction and stable transgene expression in human blood cells by a third-generation lentiviral vector. Gene Ther 10 17: 1446-57 (2003).
[45] Miyoshi H, Blomer U, Takahashi M, Gage FH, Verma IM. Development of a self-inactivating lentivirus vector. J Virol 72 10: 8150-7 (1998).
[46] Tan W, Dong Z, Wilkinson TA, Barbas CF, 3rd, Chow SA. Human immunodeficiency virus type 1 incorporated with fusion proteins consisting of integrase and the designed polydactyl zinc finger protein E2C can bias integration of viral DNA into a predetermined chromosomal region in human cells. J Virol 80 4: 1939-48 (2006).
[47] Tan W, Zhu K, Segal DJ, Barbas CF, 3rd, Chow SA. Fusion proteins consisting of human immunodeficiency virus type 1 integrase and the designed polydactyl zinc finger protein E2C direct integration of viral DNA into specific sites. J Virol 78 3: 1301-13 (2004).
[48] Philippe S, Sarkis C, Barkats M, *et al.* Lentiviral vectors with a defective integrase allow efficient and sustained transgene expression *in vitro* and *in vivo*. Proc Natl Acad Sci U S A 103 47: 17684-9 (2006).
[49] Yanez-Munoz RJ, Balaggan KS, MacNeil A, *et al.* Effective gene therapy with nonintegrating lentiviral vectors. Nat Med 12 3: 348-53 (2006).
[50] Hanawa H, Kelly PF, Nathwani AC, *et al.* Comparison of various envelope proteins for their ability to pseudotype lentiviral vectors and transduce primitive hematopoietic cells from human blood. Mol Ther 5 3: 242-51 (2002).
[51] Schauber CA, Tuerk MJ, Pacheco CD, Escarpe PA, Veres G. Lentiviral vectors pseudotyped with baculovirus gp64 efficiently transduce mouse cells *in vivo* and show tropism restriction against hematopoietic cell types *in vitro*. Gene Ther 11 3: 266-75 (2004).
[52] Kobinger GP, Weiner DJ, Yu QC, Wilson JM. Filovirus-pseudotyped lentiviral vector can efficiently and stably transduce airway epithelia *in vivo*. Nat Biotechnol 19 3: 225-30 (2001).
[53] Liu SL, Halbert CL, Miller AD. Jaagsiekte sheep retrovirus envelope efficiently pseudotypes human immunodeficiency virus type 1-based lentiviral vectors. J Virol 78 5: 2642-7 (2004).

[54] Yang L, Bailey L, Baltimore D, Wang P. Targeting lentiviral vectors to specific cell types *in vivo*. Proc Natl Acad Sci U S A 103 31: 11479-84 (2006).

[55] McNeil AC, Shupert WL, Iyasere CA, *et al.* High-level HIV-1 viremia suppresses viral antigen-specific CD4(+) T cell proliferation. Proc Natl Acad Sci U S A 98 24: 13878-83 (2001).

[56] Younes SA, Yassine-Diab B, Dumont AR, *et al.* HIV-1 viremia prevents the establishment of interleukin 2-producing HIV-specific memory CD4+ T cells endowed with proliferative capacity. J Exp Med 198 12: 1909-22 (2003).

[57] Jansen CA, De Cuyper IM, Steingrover R, *et al.* Analysis of the effect of highly active antiretroviral therapy during acute HIV-1 infection on HIV-specific CD4 T cell functions. Aids 19 11: 1145-54 (2005).

[58] Douek DC, Brenchley JM, Betts MR, *et al.* HIV preferentially infects HIV-specific CD4+ T cells. Nature 417 6884: 95-8 (2002).

[59] Rana TM. Illuminating the silence: understanding the structure and function of small RNAs. Nat Rev Mol Cell Biol 8 1: 23-36 (2007).

**Received: August 06, 2007 Revised: October 15, 2007 Accepted: October 17, 2008**

Jpn. J. Infect. Dis., 60, 106-112, 2007

**Original Article**

# Formalin-Treated UV-Inactivated SARS Coronavirus Vaccine Retains Its Immunogenicity and Promotes Th2-Type Immune Responses

Yasuko Tsunetsugu-Yokota*, Manabu Ato, Yoshimasa Takahashi, Shu-ichi Hashimoto, Tomohiro Kaji[1], Masayuki Kuraoka, Ki-ichi Yamamoto, Yu-ya Mitsuki, Takuya Yamamoto, Masamichi Oshima, Kazuo Ohnishi and Toshitada Takemori[1]

*Department of Immunology, National Institute of Infectious Diseases, Tokyo 162-8640, and [1]Immunological Memory Research Group, Riken Yokohama Institute, Kanagawa 230-0045, Japan*

(Received November 1, 2006. Accepted January 9, 2007)

**SUMMARY**: The demand for rapid and simple development of a vaccine against a newly emerging infectious disease is increasing worldwide. We previously revealed that UV-inactivated severe acute respiratory syndrome (SARS)-associated coronavirus (SARS-CoV) virions (UV-V) elicited high levels of humoral immunity and a weak Th0 response in mice immunized subcutaneously. To ensure the safety of such a whole inactivated SARS-CoV vaccine, we additionally treated the UV-V vaccine with formalin, resulting in the UV-F-V vaccine. Analysis of the immunogenicity of the UV-F-V+alum vaccine in mice revealed that it generated comparable neutralizing serum anti-SARS-CoV IgG antibody levels as the UV-V+alum vaccine. Moreover, both vaccines induced similar frequencies of anti-SARS-CoV IgG antibody-producing cells in bone marrow. Interestingly, the UV-F-V vaccine induced fewer $IgG_{2a}$ subtype antibodies and higher interleukin-4 production in vaccinated mice than did UV-V. Thus, UV-F-V imposes a Th2-type bias on the immune response, unlike UV-V. We propose here that doubly-inactivated SARS-CoV virions by UV and formalin constitute a safe vaccine that may effectively induce neutralizing antibodies in humans.

## INTRODUCTION

Severe acute respiratory syndrome (SARS)-associated coronavirus (SARS-CoV) is an etiologic agent of SARS (1,2) that originated from a coronavirus probably circulating in wild animals (3,4). The SARS-CoV genome is a single-stranded plus-sense RNA of approximately 30 kb in length containing five major open reading frames. These encode nonstructural replicase polyproteins and structural proteins, namely, the spike (S), envelope (E), membrane (M), and nucleocapsid (N) proteins (3). Angiotensin-converting enzyme 2 (ACE2) was soon identified as a cellular receptor for SARS-CoV (5). The putative S1 protein bears the extracellular domain, and amino acids 318-510 in S1 are believed to constitute the receptor-binding domain (RBD) (6). Considering that the first step in viral infection is the binding of S protein to this receptor, the S protein would be a major target for vaccination.

SARS patients develop high titers of neutralizing IgG antibodies against SARS-CoV (7) and passive transfer of SARS patient sera improves the clinical condition of newly infected patients (8). Furthermore, passive IgG transfer from immunized mice or ferrets protects naïve animals from SARS-CoV infection (9), suggesting that neutralizing antibodies mainly confer protection. Several groups have employed a variety of modern technological approaches for the development of SARS vaccines (review in [10]). These studies revealed that S protein, but not the E, M, or N proteins, protects vaccinated animals from SARS-CoV infection by inducing neutralizing antibodies (11-13) and strong cellular immunity. However, given that the vaccine studies mentioned above were largely performed in animals, which do not develop a SARS-like disease as do humans, it remains to be determined whether neutralizing anti-S antibodies will also be sufficient to protect humans from SARS.

Although the whole inactivated virion is a classic vaccine, it is more likely to induce higher levels and a broader spectrum of antibodies than recombinant viruses expressing particular sets of SARS-CoV proteins. To examine the efficacy of the whole inactivated SARS-CoV vaccine, we previously generated UV-irradiated SARS-CoV virions (UV-V) and injected this preparation subcutaneously into mice with or without alum adjuvant (14). This preparation induced high systemic levels of neutralizing anti-SARS-CoV antibodies as well as generating long-term antibody-secreting cells in the bone marrow. A low-level T-cell response was also induced in the draining lymph nodes. However, it is a fundamental requirement that any SARS vaccine developed is completely safe for humans. Consequently, in the current study, we doubly inactivated whole virions by UV-irradiation and formalin treatment. The resulting UV-irradiated and formalin-treated SARS-CoV virion (UV-F-V) preparation is presumably much safer than whole virions inactivated by UV only, and therefore this preparation was investigated in terms of its immunocompetency. We demonstrated here that relative to the UV-V preparation, UV-F-V induced comparable levels of neutralizing serum IgG and T-cell activation. Interestingly, UV-F-V promoted a Th2-type immune response with respect to IgG subtype and cytokine production patterns, unlike UV-V, which elicited a Th0 pattern of immune response.

## MATERIALS AND METHODS

**Preparation of inactivated SARS-CoV virions**: The UV-V preparation consisted of SARS-CoV (HKU39849) virions that were inactivated by exposure to 4.75J $cm^{-2}$ UV and then

*Corresponding author: Mailing address: Department of Immunology, National Institute of Infectious Diseases, Toyama 1-23-1, Shinjuku-ku, Tokyo 162-8640, Japan. Tel & Fax: +81-3-5285-1156. E-mail: yyokota@nih.go.jp

purified by sucrose density gradient centrifugation as described previously (14). We confirmed that the UV-inactivated viruses completely lost their ability to infect Vero E6 cells. Half of the purified virions were then further treated overnight in an open-capped tube with 0.02% formalin at room temperature under the laminar air flow of a biosafety cabinet. Both the formalin-treated (UV-F-V) and untreated UV-V preparations were then diluted 10-fold with PBS and re-concentrated by using an Apollo® centrifugal concentrator (150 kDa cut, Orbital Biosciences, LLC, Topsfield, Mass., USA).

**Preparation of recombinant N protein by bacteria**: The recombinant SARS-CoV N protein was prepared by using the Champion™ pET SUMO Protein Expression System (Invitrogen, Carlsbad, Calif., USA) according to the manufacturer's instructions. In this system, a His-tag and the SUMO protein (total 13 kDa) were added to the N-terminus of the N protein. We first amplified the full-length and fragments of the N gene by polymerase chain reaction (PCR) and subcloned these into a pET-SUMO expression vector. The N protein fragments were designated N1, N2, and N3 and encode the N-terminal 120, N terminal 214, and C-terminal 215 amino acids of the N protein, respectively. All recombinant proteins were purified by using Ni-NTA agarose columns (Qiagen Inc., Valencia, Calif., USA).

**Immunization of mice**: Female BALB/c mice were purchased from Nippon SLC Inc. (Shizuoka, Japan) and housed under specific pathogen-free conditions. The mouse studies were carried out according to a protocol approved by the Experimental Animal Care and Use Committee of the National Institute of Infectious Diseases. Mice at 8 weeks of age were injected subcutaneously on their back with 10 $\mu$g of UV-V or UV-F-V with or without 2 mg of alum (Pierce, Rockford, Ill., USA), and boosted by the same procedure 7 weeks after priming.

**Detection of immunoglobulins in serum samples**: Blood was obtained from the tail vein and allowed to clot overnight at 4°C. Serum samples were then treated by centrifugation. For the ELISA, microtiter plates (Dynatech, Chantily, Va., USA) were coated overnight at 4°C with SARS-CoV-infected or mock-infected Vero E6 cell lysates that had been treated with 1% NP40 and then inactivated by UV. The recombinant N proteins were also utilized as coating antigens in some experiments. After blocking, serially diluted murine serum samples were added to the plates and incubated for 2 h at 37°C. The plates were then incubated with either peroxidase-conjugated anti-mouse IgG (1:2000, Zymed, South San Francisco, Calif., USA), IgM, $IgG_1$, $IgG_{2a}$, $IgG_{2b}$ (1:2000, Zymed), $IgG_3$ (1:2000, Southern Biotechnology, Birmingham, Ala., USA) or IgA (1:2000, Southern Biotechnology) polyclonal antibodies. After 3 washes with PBS-Tween, the antibodies were detected by $o$-phenylenediamine (Zymed) at 490 nm using a Model 680 Microplate Reader (Bio-Rad, Hercules, Calif., USA). As a standard for IgG detection, pooled serum obtained from hyperimmunized mice was used and arbitrarily defined as 1000 U $ml^{-1}$, as described previously (14). The $OD_{490}$ nm value of the 100 U $ml^{-1}$ standard was approximately 0.3 in all assays.

**Neutralizing assay**: Serum samples obtained from mice immunized twice with UV-V + alum or UV-F-V + alum (at 8 weeks) were assayed for neutralizing activity as described previously (14). Neutralizing antibody titers were expressed as the minimum serum dilution that inhibited the cytopathic effect on Vero E6 cells by SARS-CoV.

**ELISPOT assay to detect antibody-producing cells**: Recombinant N proteins were diluted to 10 $\mu$g $ml^{-1}$ in PBS and then were added at 100 $\mu$l per well to plates supported by a nitrocellulose filter (Millipore, Bedford, Mass., USA). After overnight incubation of the samples at 4°C, the plates were washed 3 times with PBS and blocked overnight with 1% OVA in PBS-Tween (0.05%) at 4°C. Bone marrow cells were obtained from the femur and tibia of naïve mice. After erythrocyte lysis, single bone marrow cell suspensions were generated with RPMI 1640 supplemented with 10% FCS, $5 \times 10^{-5}$ M 2ME, 2 mM L-glutamine, 100 U $ml^{-1}$ penicillin, and 100 $\mu$g $ml^{-1}$ streptomycin; the samples were then placed on the plates at a concentration of $3 \times 10^5$ cells per well. After a 24-h cultivation period, the plates were stained with alkaline phosphatase-conjugated anti-mouse $IgG_1$ antibody (Southern Biotechnologies). Alkaline phosphatase activity was visualized by using 3-amino-ethyl carbozole and napthol AS-MX phosphate/fast blue BB (Sigma-Aldrich, St. Louis, Mo., USA).

**Western blot analysis**: Bacterial lysates containing N proteins or purified recombinant N proteins were transferred to a PVDF membrane (Genetics, Tokyo, Japan) and were then incubated with SKOT-9 monoclonal antibody (mAb) against N protein (15). After being washed, the membrane was incubated with HRP-conjugated $F(ab')_2$ fragment donkey anti-mouse IgG (H+L) (1:20,000 Jackson Immuno Research, West Grove, Pa., USA). The signal was visualized using Super Signal Western Dura Extended Duration Substrate (Pierce) and an LAS3000 Analyzer (Fuji Film, Co. Ltd., Tokyo, Japan).

**Analysis of regional T-cell responses**: Axillar and cervical lymph nodes were harvested from the mice 1 week after they had received the boost vaccination. After the single-cell suspension was prepared, the T cells were enriched with the use of a T-cell isolation kit and a magnetic cell sorting system (MACS: Miltenyi Biotec, Bergisch Gladbach, Germany). To prepare antigen-presenting cells (APCs), normal BALB/c mouse splenocytes were depleted of $Thy\text{-}1^+$ T cells by MACS and irradiated at 2000 cGy. Purified T cells (purity: 97-98%) obtained from the lymph nodes ($1 \times 10^5$ cells per well) were then cultured with the irradiated splenic APCs ($5 \times 10^5$ cells per well) in the presence or absence of UV-irradiated purified SARS-CoV virions (10 $\mu$g $ml^{-1}$). Four days after cultivation, the cytokine concentrations in the culture supernatants were measured by flow cytometry using a mouse Th1/Th2 cytokine cytometric bead array kit (Becton Dickinson, San Jose, Calif., USA), which simultaneously measured the amounts of interferon (IFN)-$\gamma$, tumor necrosis factor (TNF)-$\alpha$, interleukin (IL)-2, IL-4, and IL-5.

**Statistics**: Inter-group comparisons were performed using the one-way ANOVA followed by Tukey's post test. $P$ values of less than 0.05 were considered to be significant.

## RESULTS

**The doubly-inactivated SARS-CoV (UV-F-V) vaccine induces anti-SARS-CoV antibody levels similar to those induced by the UV-V vaccine**: Mice (five in each group) were inoculated subcutaneously with 10 $\mu$g of UV-V or UV-F-V (without or with alum) and then boosted 7 weeks later. Control mice were injected with alum only (Fig. 1). The sera were collected 4, 7, and 8 weeks after the primary vaccination, and the serum antibodies against SARS-CoV were measured by enzyme-linked immunosorbent assay (ELISA). Four weeks after the primary vaccination, the mice vaccinated with UV-V and UV-F-V had anti-SARS CoV IgG antibodies in their